63-4-4

14 February 1956

DRL-370, CF-2480
Problem UTX-2-A

DESIGN AND PERFORMANCE OF A VARIABLE GEOMETRY DIFFUSER FOR AN AXISYMMETRIC WIND TUNNEL

by

James Burley Kyser

Copy No. 66

Resulting from research done under Bureau of Ordnance Research and Development Contract NOrd 16498, Task UTX-2.

TABLE OF CONTENTS

	Page
Summary	3
Nomenclature	5
Introduction	7
General Design Considerations	9
Determination of Second Throat Area	12
Apparatus	20
Method	22
Discussion of Results	24
A. Static Pressure Tests	24
1. General Errors	24
2. Pressure Ratio Required to Start	25
3. Pressure Ratio Required to Operate	25
4. Effect of Area Ratio on Static Pressure	27
5. Static Pressure Distribution with Diffuser in Design Operating Position	28
B. Tests to Determine Length of Runs	30
1. General Error	30
2. Effect of Centerbody Location on Running Time	30
3. Effect of Test Section Obstructions on Running Time	31
Conclusions	32
References	34
List of Tables and Figures	35
Tables	36
Figures	49

DESIGN AND PERFORMANCE OF A VARIABLE GEOMETRY DIFFUSER FOR AN AXISYMMETRIC WIND TUNNEL

by

James Burley Kyser

SUMMARY

To prevent the larger second throat area required for starting a supersonic wind tunnel from penalizing the performance during the entire run, a diffuser was constructed with a movable centerbody. After the normal shock had been swallowed during starting, the centerbody was moved forward, thus constricting the flow area at the second throat. This allowed the normal shock, or shock system, to occur at a lower Mach Number, and therefore, reduced the losses.

Existing theory was not satisfactory for the solution of the flow field between the first reflection of the centerbody bow shock and the second throat, so it was assumed that this region was two-dimensional in nature. The boundary layer in this region was presumed to be unaffected by the shock reflections. Experimental data indicated that the second throat Mach Number was between 3.36 and 3.66 instead of one as predicted by the design. The magnitude of this discrepancy indicated an error in the assumption that the reflected shock waves had no effect on the boundary layer. However, even if no errors had been present, the entropy rise across the shock pattern upstream from the second throat would have prevented the Mach Number from being reduced to unity.

All tests were conducted in the 4.5-inch diameter axisymmetric tunnel of the Aeromechanics Division of Defense Research Laboratory. This tunnel is located at the Balcones Research Center of The University of Texas, Austin, Texas. The tunnel is of the intermittent-flow type with a test section Mach Number of 4.89. With the variable geometry diffuser the maximum runnin

time was 87 seconds, as compared to 30 seconds with original diffuser. However, a 0.093-inch-diameter probe extending from one wall of the test section was found to reduce the running time from the maximum of 87 seconds (with the test section empty) to 22 seconds, whereas an eighth-inch thick wedge-shaped survey rake (with 45 degree vertex angles) extending across the entire test section reduced the running time to 35 seconds. This indicates that proper model design and perhaps symmetry are as important as proper diffuser design. Since the optimum area ratio varied with the model in the test section, it was concluded that the model was an important factor that should be considered in any future diffuser design.

NOMENCLATURE

(Units as otherwise noted)

A	- cross sectional area, square inches
a	- local speed of sound, fps
C_F	- mean skin friction coefficient
C_θ	- temperature recovery factor
H	- boundary layer shape parameter
L	- characteristic length, feet
M	- Mach Number
P	- Static pressure (units noted)
P_e	- end pressure, ie, highest pressure occurring in diffuser
R	- Reynolds Number
r,η	- polar coordinates (Figure 4)
T	- temperature, degrees Rankine
t	- temperature, degrees Fahrenheit
$u,v,w,$	- velocity components, Cartesian coordinates (Figure 4)
V	- velocity, fps
V_L	- limiting velocity, fps
$v_r, v_t w$	- velocity components, polar coordinates, (Figure 4)
X,Y,Z	- Cartesian coordinates, (Figure 4)
δ	- boundary layer thickness, inches
δ^*	- boundary layer displacement thickness, inches
η_s	- shock angle, degrees
γ	- ratio of specific heats, 1.40 for air
ρ	- local density of air, slugs per cubic foot
θ	- boundary layer momentum thickness, inches

Bar over symbol denotes average conditions.

Superscripts: $( )^*$ denotes throat conditions

$( )'$ denotes reference conditions

Subscripts: $( )_0$ denotes settling chamber conditions

$( )_{1-9}$ correspond to regions defined in Figure 6

P_{01-09} denote total pressures in regions defined in Figure 6

INTRODUCTION

The procedures involved in the design of a variable geometry diffuser for an axisymmetric wind tunnel are presented in this report. Also included is a comparison of theoretical and experimental performance of the diffuser.

The diffuser was designed and constructed to replace the existing fixed geometry diffuser in the 4.5-inch test section diameter axisymmetric tunnel operated under Defense Research Laboratory Contract NOrd-9195 at the Balcones Research Center of The University of Texas in Austin, Texas. The tunnel is of the intermittent flow type and has a test section Mach Number of 4.89. With the original diffuser, runs of only 30-seconds duration could be made. This proved inadequate for obtaining certain data, so an improved diffuser was necessary for successful operation of the tunnel.

Although a diffuser cannot prevent a normal shock wave or shock system from occurring in the transition from supersonic to subsonic flow, it can reduce the Mach Number at which the normal shock occurs, and, therefore, reduce the losses resulting from the shock. While the tunnel is starting, the normal shock is located in the test section at a high Mach Number. This causes a severe entropy rise and consequently allows very little contraction in the second throat. While the tunnel is operating, the diffuser may reduce the Mach Number almost to unity before the normal shock occurs. Thus, the entropy rise is less severe, and greater contraction may be utilized.

Since a fixed geometry diffuser must have a sufficiently small contraction to allow for starting, the Mach Number at the second throat (before the normal shock) will be high enough to cause large energy losses. Therefore, in forming the second throat, a movable centerbody was used in preference to a fixed geometry diffuser. It was hoped that the higher static pressure downstream from the second throat would exert sufficient force on the centerbody to move it forward from the starting position to the operating position. This action would allow for the larger area required for starting,

without penalizing or interfering with pressure recovery throughout the
[illegible]esired automatic nature of this type of diffuser would
[illegible] tunnel such as the one in question.

[illegible] completely satisfac[illegible] procedures involved in this design. In particular, the regi[illegible] aft of the centerbody bow shock was assumed to be two-dimensional in nature, and effects of the reflected shocks on the boundary layer were neglected. Experimental data are given to help determine the validity of those assumptions and to evaluate the performance of the diffuser.

GENERAL DESIGN CONSIDERATION

It was desirable to construct the diffuser so that it could be placed in the tunnel circuit with a minimum number of changes. This required an assembly with a total length 48 inches. However, the initial 6 inches was left clear to allow for the mounting of models in the test section, and the last 8 inches was required for fastening the centerbody mount. This left 34 inches for the working section of the diffuser which obviously was insufficient for complete supersonic and subsonic diffusion. Therefore, it was decided to concentrate on supersonic diffusion and make it as efficient as possible, even at the expense of subsonic diffusion.

The initial portion of the outer shell was constructed as an extension of the existing test section, with a boundary layer displacement thickness correction of $d\delta^* / dx = 0.00814$ inches per inch as given by Reference 4. Although this value admittedly changed across each reflected shock wave, it was believed that the effect of the changes would not be great enough to alter significantly the boundary layer in the 4-inch section between the first shock reflection and the second throat. Since no theory is known to exist for the case of boundary layer-shock wave inter-action, any assumption would be strictly a guess.

A cone with a semi-vertex angle of 10 degrees, uncorrected for boundary layer growth, was selected for the nose of the centerbody. The value of 10 degrees was chosen for the semi-vertex angle because Reference 1 indicates that a larger angle would result in a far greater velocity decrease across the bow shock. This would mean a strong shock instead of a weaker one which would more nearly approach an isentropic process.

The portion of the outer shell just aft of the second throat was a 12-inch transition from the 4.838-inch-diameter test section extension to the 6.25-inch-diameter exhaust pipe. The transition section had a taper of 0.0588 inches per inch. In the region aft of the second throat, the boundary layer displacement thickness was assumed constant with a value equal to that at the second throat.

Reference 5 indicates that there should be a very slightly divergent passage just downstream from the second throat to allow subsonic flow to be completely established. Although a method of determining the length of this passage was presented, it was not utilized because it gave a length of zero for the second throat Mach Number of unity. Because of the probability that the Mach Number would not be reduced to unity at the second throat, this passage was arbitrarily made 6 inches long, diverging by about 1.5 degrees. This established a slope of 0.035 inches per inch on the centerbody for 6 inches aft of the second throat. The following 6 inches of the centerbody was cylindrical with a diameter of 4.185 inches. It was then boat-tailed and terminated abruptly due to space considerations.

The centerbody was mounted on a 27-inch length of 1.50 inch double-extra-heavy steel pipe machined to a 1.800 inch outside diameter. A collar was threaded on one end to provide a stop 5 inches forward of the designed operating position. This was done in order that contraction ratios greater than the theoretical maximum could be tested.

Six 0.625-inch diameter steel rods were welded to the mount to provide a means of bolting it in the tunnel. The center of the pipe was left open to allow the higher pressure at the downstream end to assist the motion of the centerbody from the starting to the running position. The opening in the pipe also was useful in the installation of the centerbody positioning mechanism.

Figure 18 is a schematic drawing of the diffuser assembly showing the positioning mechanism. The positioning rod shown was a 0.625-inch diameter monel tube. The centerbody static pressure taps were connected to the manometer board by plastic tubing which ran through the center of the positioning rod. Figures 19 and 20 are detail drawings of the outer shell, and the centerbody and centerbody mount assemblies. The locations of all static pressure taps are shown on these drawings, and the corresponding manometer tube numbers are indicated.

DETERMINATION OF SECOND THROAT AREA

The purpose of this section is to explain rather completely the theoretical design procedures involved in determination of the second throat area. In order to keep this section as concise as possible, derivations found in most textbooks have been ommitted. The flow in the second throat area was assumed to be composed of a viscous flow field comprising the boundary layer displacement thickness of both the centerbody and the outer shell, and a potential flow field for the remaining area. The shock waves were assumed to be reflected from the displacement thickness of the boundary layer.

POTENTIAL FLOW FIELD

The flow in the test section and test section extension was assumed to be uniform with a Mach Number of 4.89. The potential flow region here was a cylinder 4.084 inches in diameter, bounded by the displacement thickness of the boundary layer along the outer shell.

The methods for solution of the flow around a cone are presented rather completely by Ferri in Reference 1 and, therefore, will be only briefly discussed in this section. Since the limiting velocity, unlike the local speed of sound, does not change across a shock wave, the ratio of the local velocity to the limiting velocity was used frequently in this development instead of the Mach Number in order to simplify calculations. The limiting velocity is defined as the velocity that would be obtained if the flow were expanded to a zero absolute pressure. It is given by Reference 3 as:

$$V_L = 2.236\, a_o$$

For the assumed settling chamber temperature of 60°F, V_L was found to be 2504 fps.

By an iteration process, the shock angle for a 10-degree cone in a uniform flow field of Mach 4.894 was found to be 15.75 degrees. The initial point on the hodograph diagram was determined by the relation,

$$\frac{v_r}{V_L} = \frac{V_1}{V_L} \cos n_s$$

which states that the velocity component in the direction of the shock cannot change across the shock, and the relation,

$$\frac{-v_t}{V_L} = \frac{\gamma - 1}{\gamma + 1} \frac{v_r}{V_L} \cot n_s \left[\left(\frac{V_L}{v_r} \right)^2 - 1 \right]$$

which is derived from the law of conservation of energy across the shock. The values found by these equations were:

$$\frac{v_r}{V_L} = 0.877$$

$$\frac{-v_t}{V_L} = 0.1568$$

succeeding shocks was assumed to be 10 degrees in accordance with the two-dimensional theory. However, a 10-degree deflection across the shock between regions 8 and 9 was not compatible with sonic flow aft of the shock. The criterion of sonic flow was taken as the basis for establishing the properties of the shock. At the second throat, a normal shock was assumed to exist. Velocities and property values across all shock waves are given in Table 1.

The potential flow second throat area ratio, $\frac{A_1^*}{A_9^*}$, was shown to be equal to the pressure ratio, $\frac{Po_9}{Po_1}$, and had a value of 0.796. Since the nozzle throat had an area of 0.570 square inches, the potential flow second throat area was 0.716 inches.

VISCOUS FLOW FIELD

The boundary layer displacement thickness on the outer shell was taken to be that found by Harkness in Reference 4. This value was $\delta^*/x = 0.00814$ inches per inch, and its validity had been established by tests made in the tunnel.

The boundary layer displacement thickness on the cone was found by a combination of methods given in Reference 7 and 8. According to Reference 8, the local skin friction coefficient (and therefore the mean skin friction coefficient) for a cone is the same as that of a flat plate if the cone Reynolds Number is divided by 2. The representative values of $P_o = 95$ psia and $t_o = 60^\circ F$ were used to determine the Reynolds Number at the base of the cone.

Reference 1 gives the radius of curvature of the hodograph diagram as

$$\frac{R}{V_L} = \frac{\frac{v_t}{V_L} \cot n + \frac{v_r}{V_L}}{1 - \frac{2}{\gamma - 1} \frac{v_t^2/V_L^2}{1 - v_t^2/V_L^2 - v_r^2/V_L^2}}$$

Increments of about 2 degrees were taken, and the hodograph shown in Figure 5 was constructed.

Although the flow was conical in nature in region 2 (Figure 6), this was not the case in region 3. In order to avoid the complexities of an exact solution aft of region 2, an average velocity was found by the following relations:

$$\bar{u} = \frac{\Sigma \rho_i u_i^2 A_i}{\Sigma \rho_i V_i A_i} \quad ; \quad \bar{v} = \frac{\Sigma \rho_i v_i^2 A_i}{\Sigma \rho_i V_i A_i}$$

These relations state that the total momentum in the direction in question divided by the mass flow in that direction yields the average velocity. Average properties were found by assuming adiabatic compression of the flow from conditions just aft of the initial shock and corresponding to the average velocity and flow angle. This was done with the aid of the Prandtl-Meyer tables given in Reference 3.

The shock wave between regions 2 and 3 (Figure 6) was assumed to be two-dimensional in character. Prior to the shock, the average flow direction formed a 7.85-degree angle with the centerline of the tunnel. However, after the shock, the flow direction was assumed to be parallel to the center-line.

Property changes across the shock were found with the aid of shock tables given in Reference 3. The flow deflection across each of the

The Reynolds Number is

$$R = \frac{\rho V L}{\mu},$$

and the values given in Table 2 for flow at the surface of the cone are:

$$M = 4.015$$
$$\rho = 0.000418 \text{ slug/ft}^3$$
$$V = 2216 \text{ fps}$$
$$T = 124 \text{ R}^\circ$$

The viscosity was calculated by using Cope and Hartree's equation

$$\mu = \mu' \left(\frac{T}{T'}\right)^{.69}$$

where μ' and T' were taken from Reference 11 as

$$\mu' = 100 \times 10^{-7} \text{ lb - sec/ft}^2, \text{ and}$$
$$T' = 400^\circ \text{ R}$$

when these values were substituted into the Cope and Hartree equation, the result was $\mu = 35.3 \times 10^{-7}$ lb - sec/ft^2 = 1.10×10^{-7} slug/ft sec. The mean skin friction coefficient was evaluated at the base of the cone where L = 0.953 feet. This gave a Reynolds Number of 8,030,000 which was equivalent to a flat plate with a Reynolds Number of 4,015,000.

Wilson, in Reference 7, gives the relation between mean skin friction coefficient and Reynolds Number as:

$$\frac{\sin^{-1}\sqrt{\sigma}}{\sqrt{\sigma}}\left(1 + C_\theta \frac{\gamma - 1}{2} M_1^2\right)^{-\frac{1}{2}} \frac{0.242}{\sqrt{C_F}} =$$

$$\log_{10}(C_F R) - 0.768 \log_{10}\left[\left(1 + C_\theta \frac{\gamma - 1}{2} M_1\right)^2\right]$$

where:

$$\sigma = \frac{\left[\frac{(\gamma - 1)}{2}\right] M_1^2}{1 + \frac{(\gamma - 1)}{2} M_1^2}$$

An experimental value of the temperature recovery factor (used in Reference 7) of $C_\theta = 0.88$ was substituted into the equation along with the variables given above, and the result of $C_F = 0.00214$ was obtained.

This value of C_F was converted to the corresponding displacement thickness by the following fundamental relations:

$$C_F = 2\frac{\theta}{X}$$

and

$$\frac{\delta^*}{X} = H\frac{\theta}{X}.$$

Therefore

$$\frac{\delta^*}{X} = \frac{H}{2} C_F .$$

The shape parameter H, was given by Reference 6 as $H = 8.418$ for a Mach Number of 4.015. The value of $\frac{\delta^*}{X}$ was then found to be $\frac{\delta^*}{X} = 0.0090$.

Although the values of $\frac{\delta^*}{X}$ for the cone and outer shell were admittedly not constant along the entire surface, they were assumed so in order to avoid complex machining procedures. Also, it was felt that the errors introduced by this procedure would be small, due to the fact that distances between the first shock wave reflection through each boundary layer and the normal shock were small.

DETERMINATION OF THE TOTAL AREA

The total displacement thickness for the boundary layer on the outer shell was 0.389 inches. This was the result of a 0.00814 inch per inch growth over a length of 46.6 inches. This gave a flow region with an outside diameter of 4.084 inches. Therefore, the area was 5.283 square inches.

As already mentioned, the potential flow second throat area was 0.716 square inches. Since this area was annular in form, with an outside diameter of 4.084 inches, the inside diameter was 3.971 inches.

The value of 3.971 inches was the diameter of the base of the 10-degree cone uncorrected for boundary layer. This base diameter therefore set the length of the uncorrected cone to be 11.25 inches. When the boundary layer correction of 0.0090 inches per inch was subtracted from the slope of the surface of the cone, the base diameter became 3.765 inches. This left an equivalent annular viscous flow region for the cone with an outside diameter of 3.991 inches and an inside diameter of 3.765 inches. The area was 1.252 square inches.

The total second throat area was composed of the three regions above and had a value of 7.25 square inches.

AREA REQUIRED FOR STARTING

While starting, it was assumed that the normal shock occurred in the test section at a Mach Number of 4.894. At the second throat, the velocity was taken as a fully developed seventh root profile with a maximum Mach Number of unity occurring midway between the surface of the cone and the surface of the outer shell.

According to Reference 11, the ratio of critical areas across a normal shock at Mach 4.894 is 0.0667. The nozzle throat area of 0.570 square inches was divided by this value to give the uncorrected second throat area of 8.546 square inches. At the second throat the Mach Number was unity, if the previous assumptions were correct. The values of the boundary layer shape parameters, H and $\frac{\delta}{\theta}$, given by Reference 6 for a Mach Number of unity are

$$H = 1.734$$

$$\frac{\delta}{\theta} = 10.984$$

Therefore,

$$\frac{\delta^*}{\delta} = \frac{\delta^*}{\theta} \times \frac{\theta}{\delta} = H \times \frac{1}{\frac{\delta}{\theta}} = 0.1579$$

Since it was assumed that the entire passage at the second throat was filled with boundary layer, the uncorrected area was 84.21% of the total cross sectional area. The uncorrected area of 8.546 square inches was divided by 0.8421 to yield a total area of 10.15 square inches. Therefore, the centerbody retraction for starting was 3.136 inches.

APPARATUS

Tests were conducted in the 4.5-inch axisymmetric wind tunnel at the Balcones Research Center in Austin, Texas. This is an intermittent flow tunnel with a test section Mach Number of 4.89. Figure 1 shows the tunnel circuit between the nozzle (at the extreme left) and the 6-inch pipe to the vacuum tank (at the extreme right). The diffuser assembly was installed as a permanent part of the circuit just aft of the test section, placing the front lip of the diffuser 26.6 inches from the nozzle throat and the second throat 46.6 inches from the nozzle. For clarity, in Figure 1 the outer shell is suspended below its installed position.

The high pressure system consisted of a 100-hp four-stage air compressor with a capacity of 144 cubic feet per minute (at standard conditions) and a delivery pressure of 3000 psi. Four tanks with a total volume of 100 cubic feet made up the high pressure reservoir. The low pressure system was composed of a 2000 cubic foot vacuum tank which was exhausted to a minimum absolute pressure of 0.5 inches of mercury by five 3-hp pumps. Approximately 20 minutes was required for the vacuum pumps to lower the vacuum tank pressure from shutdown pressure to 1 inch of mercury.

The settling chamber pressure was controlled by a quick opening automatic pressure regulating valve, which throttled the high pressure air from reservoir conditions to the desired P_o. Settling chamber pressure was measured by a pressure gauge with an 18-inch face, shown at the extreme right in Figure 2. This allowed measurements to within 0.5 psi. Settling chamber temperature was given by a thermistor installed just ahead of the nozzle.

The centerbody was positioned by an indicator fastened to the positioning rod and a scale bolted to the tunnel support frame. This may be seen at the extreme right of Figure 1. A stop was provided on the positioning rod to prevent travel forward of the desired centerbody location. This allowed the centerbody to be retracted for starting, and the forward thrust kept the centerbody fast against the stop at all times during the run after the normal shock had been swallowed.

METHOD

Static pressure taps were located along the entire shell at intervals varying from 0.2 inches near the second throat, to 4 inches at the extreme rear. Static pressure taps were also placed along the conical portion of the centerbody. A total of 27 taps, 22 on the shell and 5 on the centerbody, was installed in the diffuser. Table 4 gives the exact location of all the taps. The static pressure taps were connected to a 50-tube manometer board shown to the left of center in Figure 2. Data were recorded by a photograph taken of the manometer board each run at the time that the normal shock wave was located in the second throat. Figure 3 is a typical photograph of the manometer board, taken during a run with the centerbody in design operating position.

Runs were made with the centerbody near starting position, near the design operating position, and in the most forward position. In each case, a photographic record was made of the manometer board. Running time, P_o, and T_o were also recorded.

To determine the effects of the test section obstructions on the performance of the diffuser, runs were made with a probe, a survey rake, and a flat plate in the test section. The shank of the probe was a 0.095-inch diameter tube, and the effects of three different depths of penetration were determined. The survey rake was approximately 1/8 of an inch thick and 3/4 of an inch wide, with front and rear total included angles of 60 degrees. It extended across the entire diameter of the test section. The flat plate was 90 inches long, 3/8 of an inch thick, and also extended across the test section. For each condition, the optimum centerbody location was found, and the running time for this position was recorded.

An attempt was made to determine the value of $\frac{P_o}{P_e}$, the pressure ratio required to operate. This was done by exhausting into the atmosphere and manually raising the settling chamber pressure to that required to start. However, the construction of the pressure regulating system prohibited pressures greater than 300 psig, which was not enough to start the tunnel.

DISCUSSION OF RESULTS

A. Static Pressure Tests

1. General Errors

All data taken during these tests were subject to certain inherent sources of error. One of these was the effect of propagation of disturbances by the boundary layer. The subsonic portion of the boundary layer may, by this effect, permit pressure disturbances to be propagated upstream in an otherwise supersonic flow. Also, a small error in measuring static pressure may cause a serious error in Mach Numbers indicated by pressure data.

Another source of error stemmed from the time required for the manometer board to stabilize. Since static pressures aft of the second throat increased continuously during the run, it may be expected that recorded data did not accurately represent the existing static pressures. To help correct this condition, several sets of data were taken for most centerbody locations while the normal shock wave was in different positions. Pressures upstream from the second throat were taken from data recorded while the normal shock was located slightly downstream of the second throat, and the pressures downstream from the second throat were taken from data recorded a second or so after the normal shock had passed through the second throat.

Preliminary runs showed that the diffuser was very sensitive to the symmetry of the system, and therefore it was deduced that a slight eccentricity in the centerbody alignment might seriously alter the diffuser performance. To check centerbody alignment, runs were made with it rotated 90 degrees and 180 degrees clockwise. Since no effect of the rotation could be detected from static pressure data, it was assumed that the alignment was sufficiently correct.

2. Pressure Ratio Required to Start

Since the construction of the pressure regulating valve prevented settling chamber pressures higher than about 300 psig, the tunnel was never able to start while exhausting into atmosphere. Reference 5 indicates that the minimum pressure ratio required to start the 1.5-inch two-dimensional tunnel reported on was about 21 at an area ratio of 1.35. This indicates that the tunnel described in this report may start with a pressure ratio slightly higher than the maximum value of 22.6 obtained in these tests. With the previous diffuser, the tunnel could start with a pressure ratio of about 19 at an area ratio of 1.35. The better starting performance of the original diffuser was in part due to the shorter distance between the test section and the second throat, 6 inches as compared to 26 inches on the variable geometry diffuser. This meant far less skin friction drag. Since the diffuser acts as a subsonic diffuser while the tunnel is starting, the original installation with its 3-foot slightly divergent channel was undoubtedly more effective than the variable geometry diffuser with its 6-inch slightly divergent section.

3. Pressure Ratio Required to Operate

The best measure of the performance of a diffuser is the pressure ratio, P_o/P_c, required to operate the tunnel circuit. Figure 7 shows the effect of area ratio at the second throat on pressure ratio required to operate. Also included are data from the most efficient run reported in Reference 5. The curves are displaced from one another because the viscosity effects are more pronounced in a smaller tunnel such as the one used by Goldbaum (Reference 5).

Since wind tunnel tests are seldom made with empty test sections, it is important to have some knowledge of the diffuser performance while obstructions are present in the test section. Therefore, runs were made

with a 0.095-inch diameter probe, a survey rake, or a 9.0-inch flat plate installed in the test section. The probe had little effect on the over-all performance when extended only an inch from the wall. However, when it was extended 1.75 inches and 2.5 inches, the pressure ratio required to operate the tunnel was more than doubled. This indicates a serious flaw in the operation of axisymmetric tunnels. The rake, which extended across the entire test section had little more effect than the probe when extended 1.75 inches (approximately 40% of the distance across the tunnel). This may have been caused by the strong, detached bow shock from the circular cross section of the probe while the wedge-shaped leading edge of the rake created a much weaker attached shock. The second throat area ratio of 1.20 with the diffuser in the fully retracted position, approximately 6 inches rearward of design operating position, was too great to permit the shock to be swallowed while the flat plate was installed. Therefore, little can be said about tunnel performance with this model in the test section. Figure 17 gives static pressures as a function of the distance from the nozzle. It shows that the normal shock is located somewhere between the end of the test section and the front of the centerbody. Static pressure data from the pressure taps on the flat plate appear to be unaffected by the fact that the normal shock had not been completely swallowed.

The data used in plotting the curve shown in Figure 7 were not obtained by direct measurement and, therefore, should not be considered exact. Because of difficulties encountered in accurately measuring vacuum tank pressure at shutdown, the following procedure was used to obtain data shown in Figure 7. Running time and centerbody position could be measured with a reasonable degree of accuracy so Figure 8 was used as the basis for this analysis. The centerbody locations for the data shown in Figure 8 were converted into second throat area ratios by means of Figure 9.

Since the pressure aft of the second throat were constantly dropping, the manometer board lag time prevented accurate readings from being made at

the instant the shock popped through the second throat. The vacuum pumps lowered the vacuum tank pressure some during the time required for the manometer board to stabilize after shutdown; this prevented an accurate reading of P_c from being made after shutdown. To correct this condition, pressure readings were taken both before and after shutdown. These data were plotted in Figure 10 as running time, vs., shut-down pressure ratio, P_c/P_o. The point at zero running time was calculated by assuming an initial vacuum tank pressure of one inch of mercury and a settling chamber pressure of 94.9 psia, or 82.5 psig. A smooth curve was drawn through these data points, and it was assumed that the curve, not the data, was correct. The running time of the data shown in Figure 8 were converted into pressure ratios by means of Figure 10. The values thus obtained were plotted as area ratio, A/A_g, vs. pressure ratio, P_o/P_c, to yield Figure 7. This procedure assumed that vacuum tank temperature was a function of time only, and was not affected by the centerbody location or by a model in the test section.

4. Effect of Area Ratio on Static Pressure

Figures 11, 12, 13, and 14 show the effect of area ratio on static pressure. A wide scatter of data points in the region ahead of the second throat was evidenced in all cases. This was caused by the shock pattern, since points on the shell and on the cone occurring at the same area ratio were separated by a shock wave and hence, had different static pressures. All curves have approximately the same form, but are displaced, and changed in size according to the maximum area ratio. Figure 11 shows all pressure data plotted in non-dimensional form. For each centerbody setting, the local pressure data were divided by the second throat area to yield the contraction ratios. Figure 12 illustrates the gain in pressure recovery that was obtained by making the centerbody movable. The data correspond to the optimum operating position (centerbody 4.88 inches forward of design operating position), the maximum area ratio that would allow starting (centerbody 2.75 inches rearward of design operating position), and design starting

position (centerbody 3.03 inches rearward of design operating position). Also included in Figure 12 is the curve from Figures 13 and 14. Figure 13 shows data from runs made with the centerbody located 0.1 inch forward and 0.1 inch rearward of the design operating position, while Figure 14 shows data from runs made with the centerbody in design operating position. The proximity of data from these runs illustrates that pressure data were not greatly affected by small changes in centerbody location.

In all cases, the area ratio was defined as the mean test section area, 15.50 square inches, divided by the area in question. This was done to be consistent with data presented in Reference 5.

Although the maximum pressure recovery reported was obtained with the centerbody located 4.88 inches ahead of design operating position, it was not proved that this area ratio gave the best possible pressure recovery. However, since the centerbody was at the forward end of its travel in this position, tests could not be made with greater area ratios.

5. Static Pressure Distribution with Diffuser in Design Operating Position

The agreement between theoretical and measured static pressure data was quite good in front of the bow shock from the centerbody. However, this was not true aft of the bow shock. Discrepancies start immediately aft of the bow shock and grow progressively worse downstream. This was anticipated due to the fact that the theory did not take into account either the entropy rise or the energy loss due to viscous friction in the boundary layer. Figure 15 gives the static pressure ratio, P/P_o, along the entire length of the diffuser shell and along the conical portion of the centerbody, and Figure 16 gives the area ratio along the entire length of the diffuser. At the second throat, the static pressure ratio is 0.0085 on the shell and 0.0125 on the centerbody. If the pressure is assumed to vary linearly across the second throat, an average pressure ratio of 0.0105 is established.

Since the compression process between regions 1 and 9 (Figure 6) lies somewhere between an isentropic compression and one obtained across a single strong shock, it is possible to calculate an approximate second throat Mach Number from static pressure data. The isentropic Mach Number, i.e. that Mach Number corresponding to an isentropic expansion from the settling chamber pressure to the pressure in question, for the second throat was found to be 3.66. The ratio of second throat pressure to test section pressure was 4.96, which established the hypothetical shock angle as 25.4 degrees. This, in turn, established the flow deflection to be 15.8 degrees, and, therefore, the Mach Number was 3.36. It may be then concluded that the second throat Mach Number was between 3.35 and 3.66.

Equating the mass flow through the nozzle throat to the mass flow through the second throat, and assuming an isentropic compression, the potential flow second throat area required was found to be 4.49 square inches. Similarly, assuming compression by one strong shock, the potential flow second throat area required was found to be 5.00 square inches. Since the total second throat area was 7.25 square inches, the total area occupied by the boundary layer displacement thickness on the centerbody and shell was between 2.74 square inches and 2.25 square inches. Since nothing is known about the actual distribution of the boundary layer between the cone surface and the shell surface, this is the furthermost point to which this approximate analysis can be carried. However, it appears that the assumption of constant boundary layer growth after reflected shocks caused far greater error when applied to the shell than when applied to the centerbody.

An attempt was made to determine the diffuser shock pattern. It was impossible to establish the exact location of each shock reflection because of the tendency of the boundary layer to transmit pressure disturbances upstream. Figures 14 and 15 clearly show the effect of a shock pattern aft of the second throat. This shock pattern appears to retain full strength

for about 9 inches, whereupon it gradually decreases in strength and ceases in about 5 more inches. This indicated that the 6-inch slightly divergent passage was not sufficient to allow complete transition to subsonic flow. Aft of this, the pressure drops off gradually, either as a result of viscous drag in the boundary layer or as a result of drag from the centerbody support.

B. Tests to Determine Length of Runs

1. General Errors

All tests were made with an initial vacuum tank pressure of approximately one inch of mercury and a settling chamber pressure of 82.5 psig. Running time was started when the valve started opening and ended when the shock popped through the second throat. When the centerbody was located several inches ahead of design operating position, this made a very audible disturbance. However, when the centerbody was retracted, it was very difficult to tell when the shock popped through the second throat. This introduced a possible source of error of several seconds on the shorter runs. Also present was the possibility that small leaks in the system might cause boundary layer thickening in the region aft of the leak and create a reduction in diffuser efficiency. This would, in turn, cause a reduction in running time. Since it was improbable that all leaks in the system were completely eliminated, all values of running time were undoubtedly subject to this error.

2. Effect of Centerbody Location on Running Time

Figure 8 shows the effects of centerbody location on running time. All data were taken with the vacuum pumps operating during the entire run. Reference 5 indicates that the curve would break sharply downward if the

optimum area ratio were exceeded. However, the construction of the centerbody prevented tests with area ratios greater than 3.03 from being conducted. The maximum deviation of points from the line was about 4% This was less scatter of points than was expected, considering the accuracy of the measurements.

3. Effects of Test Section Obstructions on Running Time

Since vacuum tank pressure varies approximately linearly with the length of the run (Figure 10), the remarks made about the effects of the test section obstructions on pressure ratio required to operate apply here, also. The running times with the probe extended 1.75 inches and 2.5 inches into the test section were so short as to make it questionable whether or not probe data could be obtained. The remedy probably lies in the redesign of the probe, i.e. use of a double wedge cross section, instead of a redesign of the diffuser.

CONCLUSIONS

The theory used in the design of this diffuser predicted a Mach Number of unity at the second throat instead of the value between 3.36 and 3.66 indicated by static pressure data. This discrepancy was caused partially by the entropy rise in the boundary layer and partially by an error in the predicted boundary layer growth. Previous total pressure surveys indicated that the boundary layer correction of $dS^*/dx = 0.00814$ applied to the surface of the nozzle and test section was correct. Therefore, it may be assumed that this correction was valid along the entire region between the nozzle and the first reflection of the bow shock from the centerbody. Since the thickness of the boundary layer on the centerbody was not large enough to cause an error of the observed magnitude, it appears that the growth of the displacement thickness of the boundary layer on the outer shell was less than the assumed rate of increase after the first reflected shock. However, the exact behavior of the boundary layer in the region aft of the shock reflection could have been found only by extensive boundary layer surveys, which time did not permit.

In spite of the limitations of the theory used in this design, fairly good results were obtained. Figure 8 illustrates that the design centerbody location appears to be the best for either the 0.095-inch diameter probe or the survey rake used in these tests. However, with the flat plate installed, supersonic flow could not be established in the entire region ahead of the second throat. This indicates the need of a smaller centerbody or a reduction of the distance between the test section and the second throat to reduce losses from viscous friction.

The pronounced effect of test section obstructions on optimum area ratios indicates that no single diffuser design will be best for all model configurations. However, a great gain in running time, may be obtained by use of models that are smaller than those used in these tests.

Throughout the tests, the centerbody was positioned manually. It was retracted to the starting position and advanced once the shock had been swallowed. Although the forward thrust on the centerbody varied according to the centerbody position and the model in the test section, it was at all times more than that required to overcome the friction in the pressure seal on the positioning rod. However, since the forward thrust was found to be sufficient to force the centerbody far enough forward to choke the tunnel, a stop must be provided if the operation is to be fully automatic.

This report has been distributed in accordance with
the list for Aerodynamics contained in APL/JHU, TG 8 - 11, dated November, 1953.

REFERENCES

1. Ferri, A., Elements of Aerodynamics of Supersonic Flows, New York, The Macmillan Co., Inc., 1949.

2. Kuethe, A. M., and Schetzer, J. D., Foundations of Aerodynamics, New York, John Wiley and Sons, Inc., 1950.

3. Liepmann, H. W., and Puckett, A. E., Introduction to Aerodynamics of a Compressible Fluid, New York, John Wiley and Sons, Inc., 1943.

4. Harkness, John L; "The Design of a Three Dimensional Intermittent Flow Hypersonic Wind Tunnel", Report Number DRL - 197, Austin, Texas, Defense Research Laboratory, The University of Texas, 1949.

5. Goldbaum, George C., "Comparison of Theoretical and Experimental Performance of A Variable Geometry Diffuser at a Mach Number of 5.0," Report Number DRL - 331, Austin, Texas, Defense Research Laboratory, The University of Texas, April, 1951.

6. "Aerodynamic Characteristics of Nozzels and Diffusers for Supersonic Wind Tunnels," Report Number DRL - 281, Austin, Texas, Defense Research Laboratory, The University of Texas, April, 1951.

7. Wilson, Robert E., "Turbulent Boundary Layer Characteristics at Supersonic Speeds - Theory and Experiment," Journal of the Aeronautical Sciences, Volume 17, Number 9, September, 1950.

8. Van Driest, E. R. "Turbulent Boundary Layer on a Cone in a Supersonic Flow at Zero Angle of Attack", Journal of the Aeronautical Sciences, Volume 19, Number 1, January, 1952.

9. "Handbook of Supersonic Aerodynamics," Navord Report Number 1488, Volumes 1 and 2, Washington, D. C., Bureau of Ordnance, 1950.

10. Burington, R. S., Handbook of Mathematical Tables and Formulas. Sandusky, Ohio, Handbook Publisher, Inc., 1948.

11. Keenan, J. H. and Kaye, J., Gas Tables, New York, John Wiley and Sons, Inc., 1948.

LIST OF TABLES AND FIGURES

Table I : Theoretical Shock Characteristics
Table II : Theoretical Flow Characteristics
Table III : Reduced Data
Table IV : Location of Static Pressure Taps
Figure 1 : Photograph of Diffuser Assembly
Figure 2 : Photograph of Tunnel Working Section and Instruments
Figure 3 : Typical Photograph of Manometer Board
Figure 4 : Coordinate Systems
Figure 5 : Hodograph of Flow in the Conical Regions
Figure 6 : Predicted Shock Pattern
Figure 7 : Effect of Area Ratio at the Second Throat on Pressure Ratio Required to Operate
Figure 8 : Effects of Centerbody Location on Running Time
Figure 9 : Area Ratio vs. Centerbody Location
Figure 10 : Effect of Running Time on End Pressure Ratio
Figure 11 : Pressure Recovery Ratio vs. Contraction Ratio
Figure 12 : Pressure Ratio vs. Area Ratio (Centerbody retracted 3.03 inches, retracted 2.75 inches, and advanced 4.88 inches)
Figure 13 : Pressure Ratio vs. Area Ratio (Centerbody retracted 0.1 inch and advanced 0.1 inch)
Figure 14 : Pressure Ratio vs Area Ratio (design operating position)
Figure 15 : Pressure Ratio and Mach Number along Length of Diffuser (design operating position)
Figure 16 : Area Ratio Along Length of Diffuser (design operating position)
Figure 17 : Pressure Ratio Along Length of Diffuser (with flat plate in test section)
Figure 18 : Schematic Drawing of Positioning Mechanism
Figure 19 : Detail Drawing of Outer Shell
Figure 20 : Detail Drawing of Centerbody and Mount

TABLE I THEORETICAL SHOCK CHARACTERISTICS

Shock Wave Location (Fig. 6)	Mach No. Before Shock	Mach No. After Shock	Shock Angle Deg	Static Press. Ratio P_n/P_{n-1}	Total Press. Ratio P_{on}/P_{on-1}	Temperature Ratio T_n/T_{n-1}	Density Ratio ρ_n/ρ_{n-1}
I - II	4.89	4.37	15.75	1.89	.974	1.21	1.56
II - III	4.18	3.59	11.8	2.153	.956	1.26	1.71
III - IV	3.59	2.99	23.[illegible]	2.32	.924	1.29	1.7[illegible]
IV - V	2.99	2.49	[illegible]	2.01	.966	1.23	1.6[illegible]
V - VI	2.49	2.08	32.0	1.89	.976	1.20	1.52
VI - VII	2.08	1.72	27.8	1.73	.983	1.18	1.47
VII - VIII	1.72	1.36	46.7	1.65	.989	1.15	1.42
VIII - IX	1.36	1.00	53.9	1.58	.990	1.14	1.38

TABLE II THEORETICAL FLOW CHARACTERISTICS

Region (Fig. 5)	Mach Number	Velocity FPS	Static Pressure Psi	Static Press. Ratio $\frac{P}{P_o}$	Density Slug/ft^3	Density Ratio	Tempt. ^oR	Tempt. Ratio $\frac{T}{T_o}$	Total Pressure Ratio $\frac{Pon}{P_c}$
Settling Chamber	0	0	95.800		.01549		520		1.000
1	4.00	2284	.205	.00214	.000192	.0124	89.4	.172	.974
2 (=15.5)	4.37	2231	.387	.00404	.000330	.0214	108	.208	.974
2 (=14)	4.24	2226	.451	.00471	.000356	.0297	113	.218	.974
2 (=12)	4.13	2221	.523	.00546	.000358	.0231	118	.227	.974
2 (=10)	4.01	2216	.615	.00642	.000418	.0270	124	.238	.974
2	4.18	2224	.492	.00514	.000355	.0230	116	.223	.931
3	3.59		1.06	.0111	.000607	.0392	147	.282	.877
4	2.99		2.46	.0256	.00109	.0703	189	.364	.847
5	2.69		4.95	.0516	.00181	.117	235	.448	.827
6	2.08		9.33	.0974	.00274	.177	280	.538	.813
7	1.72		17.9	.188	.00404	.261	330	.634	.804
8	1.36		26.6	.277	.00575	.371	379	.729	.796
9	1.00		41.62	.434	.00906	.585	432	.831	

A_o = 1125 F. P. S.

TABLE III REDUCED DATA

Part 1. CENTERBODY AT DESIGN OPERATING POSITION

TEST SECTION EMPTY

Station (Tap No.)	Distance From Front Lip-in.	Average Reading	Static Pressure in.hg.abs.	$\frac{P}{P_o}$	M_1	$\frac{P}{P_e}$	Area	$\frac{A_1}{A}$	$\frac{A_9}{A}$
21	3.00	38.86	.403	.002067	4.924	.0281	16.339	.949	.443
22	6.00	38.85	.413	.002118	4.904	.0298	16.691	.929	.434
23	9.00	38.84	.423	.002170	4.883	.0306	17.035	.910	.426
24	11.00	38.86	.403	.002067	4.924	.0281	16.837	.921	.431
44*	12.00	38.40	.863	.004226	-----	.0595	16.473	.941	.440
25	13.00	38.85	.413	.002118	4.904	.0298	15.931	.973	.466
26	15.00	38.86	.403	.002067	4.924	.0281	14.330	1.082	.507
45*	15.00	38.40	.863	.004226	-----	.0595	14.330	1.082	.507
27	16.90	38.30	.963	.004940	-----	.0696	12.155	1.275	.596
28	17.80	38.01	1.253	.006529	-----	.0920	10.883	1.424	.667
46*	17.80	38.33	.933	.004785	-----	.0673	10.883	1.424	.667
29	19.37	37.80	1.463	.007504	-----	.1057	8.379	1.850	.866
47*	19.64	37.05	2.203	.01130	-----	.1590	7.878	1.968	.921
30	19.84	37.80	1.463	.007485	-----	.1053	7.541	2.055	.962
48*	19.925	36.68	2.583	.01325	-----	.1865	7.365	2.105	.985
31	20.00	Second Throat-----		------	-----	-----	7.249	2.138	1.000
32	21.00	36.10	3.163	.01620	-----	.228	7.740	2.003	.937
33	22.00	35.92	3.343	.01712	-----	.241	8.236	1.882	.881
34	23.00	33.76	5.503	.02818	-----	.396	8.753	1.771	.829
35	25.00	31.50	7.763	.03975	-----	.528	9.824	1.578	.738
36	27.00	29.04	10.223	.05235	-----	.738	11.423	1.357	.635
37	29.00	26.92	12.343	.06320	-----	.888	13.557	1.143	.535
38	31.00	26.22	13.043	.06679	-----	.940	15.776	.983	.460
39	34.00	25.50	17.763	.07047	-----	.991	22.872	.678	.317
40	37.00	25.38	13.883	.07109	-----	1.000	28.182	.550	.257
41	42.00	25.50	13.763	.07047	-----	.991	28.182	.550	.257
42	46.00	25.60	13.663	.06996	-----	.985	28.182	.550	.257

Second Throat Area = 7.249 Square Inches.
In Front of Second Throat, P_o = 95.73 psia, Reference = 39.263 inches.
Behind Second Throat. P_o = 95.90 psia. Reference = 39.263 inches.

* Pressure Taps on Centerbody.

Part 2. CENTERBODY RETRACTED 3.03 INCHES FROM DESIGN OPERATING POSITION

TEST SECTION EMPTY

Station	Average Reading	Static Pressure in.hg.abs.	$\frac{P}{P_o}$	$\frac{P}{P_e}$	Area in ^{2}	$\frac{\bar{A}_1}{A}$	$\frac{A_2}{A}$
21	38.80	.418	.00218	.0415	16.40	.945	.607
22	38.80	.418	.00218	.0415	16.69	.929	.596
23	38.80	.418	.00218	.0415	17.04	.910	.584
24	38.80	.418	.00218	.0415	17.28	.897	.575
25	38.80	.418	.00218	.0415	17.19	.902	.578
26	38.80	.418	.00218	.0415	16.78	.924	.593
44*	38.39	.828	.00432	.0822	16.76	.925	.594
27	38.80	.418	.00218	.0415	15.73	.985	.632
28	38.80	.418	.00218	.0415	14.92	1.039	.667
45*	38.40	.418	.00426	.0810	14.68	1.056	.678
29	38.77	.448	.00234	.445	13.23	1.172	.753
30	38.52	.698	.00364	.0693	12.61	1.229	.789
31	38.52	.698	.00364	.0693	12.35	1.255	.806
32	38.38	.838	.00436	.0828	11.77	1.317	.845
33	38.19	1.028	.00536	.1020	11.00	1.409	.905
46*	38.42	.798	.00416	.0812	10.85	1.429	.918
47*	38.60	.618	.00322	.0613	10.37	1.495	.962
48*	38.72	.498	.00260	.0495	10.10	1.535	.989
34	37.74	1.478	.00770	.1467	10.10	1.535	.989
35	35.97	3.248	.01693	.322	11.18	1.386	.893
36	34.95	4.268	.02225	.423	12.28	1.262	.813
37	33.72	5.498	.02866	.546	13.50	1.067	.687
38	32.50	6.718	.03502	.677	15.72	.986	.635
39	30.50	8.718	.04544	.865	16.85	.920	.592
40	29.34	9.878	.05149	.980	27.50	.564	.363
41	29.14	10.078	.05253	1.000	28.18	.550	.354
42	29.31	9.908	.05165	.983	28.18	.550	.354

Second Throat Area = 9.98 Square Inches

Reference = 39.218

P_o = 94.40 psia

* Pressure Taps on Centerbody

Part 3. CENTERBODY RETRACTED 2.75 INCHES FROM

DESIGN OPERATING POSITION

TEST SECTION EMPTY

Station	Average Reading	Static Pressure in.hg.abs.	$\frac{P}{P_o}$	$\frac{P}{P_e}$	Area in^2	$\frac{\bar{A}_1}{A}$	$\frac{A_2}{A}$
21	38.79	.429	.00219	.0408	16.40	.945	.648
22	38.80	.421	.00214	.0400	16.69	.929	.632
23	38.79	.427	.00219	.0408	17.04	.910	.619
24	38.79	.427	.00219	.0408	17.38	.898	.611
25	38.78	.437	.00224	.0418	17.36	.893	.608
26	38.80	.417	.00214	.0400	17.04	.910	.619
44*	38.32	.897	.00465	.0942	16.85	.920	.627
27	38.80	.417	.00214	.0400	16.32	.950	.647
28	38.80	.417	.00214	.0400	15.65	.990	.674
45*	38.35	.867	.00444	.0828	14.78	1.049	.715
29	38.58	.637	.00326	.0608	14.15	1.095	.746
30	38.42	.797	.00408	.0762	14.62	1.142	.778
31	38.42	.797	.00408	.0762	13.40	1.157	.788
32	38.28	.937	.00480	.0896	12.90	1.202	.819
46*	38.40	.817	.00418	.0781	12.53	1.237	.844
33	38.10	1.117	.00572	.1068	12.21	1.269	.865
34	37.30	1.917	.00981	.1830	11.44	1.354	.923
47*	38.60	.617	.00316	.0589	11.10	1.396	.951
48*	38.50	.717	.00367	.0701	10.68	1.451	.989
35	35.80	3.417	.01749	.326	11.48	1.350	.920
36	34.60	4.617	.02364	.441	12.61	1.229	.838
37	33.22	5.997	.03070	.572	13.89	1.116	.760
38	31.94	7.277	.03726	.696	15.77	.983	.670
39	29.95	9.267	.04745	.885	16.85	.920	.627
40	28.88	10.337	.05292	.988	21.50	.721	.491
41	28.74	10.477	.05364	1.000	28.18	.550	.375
42	28.82	10.397	.05323	.993	28.18	.550	.375

Second Throat Area = 10.56 Square Inches
Reference = 39.217
P_o = 95.90 psia

*Pressure Taps on Centerbody

Part 4. CENTERBODY RETRACTED 0.1 INCH FROM DESIGN OPERATING POSITION

TEST SECTION EMPTY

Station	Average Reading	Static Pressure in.hg.abs.	$\frac{P}{\bar{P}_o}$	$\frac{P}{\bar{P}_e}$	Area	$\frac{\bar{A}_1}{A}$	$\frac{A_2}{A}$
21	38.83	.403	.00216	.0301	16.34	.949	.457
22	38.83	.403	.00216	.0301	16.69	.929	.437
23	38.82	.413	.00221	.0307	16.98	.913	.430
24	38.82	.413	.00221	.0307	16.68	.929	.437
44*	38.38	.853	.00447	.0621	16.40	.945	.445
25	38.83	.403	.00216	.0301	16.03	.967	.455
26	38.83	.403	.00216	.0301	14.44	1.073	.505
45*	38.39	.843	.00442	.0613	14.35	1.080	.508
27	38.31	.923	.00483	.0652	12.03	1.288	.607
28	38.02	1.213	.00631	.0876	11.03	1.405	.662
46*	38.44	.793	.00416	.0578	10.87	1.426	.672
29	37.80	1.433	.00744	.1035	8.58	1.807	.851
47*	37.10	2.133	.01092	.1528	7.90	1.962	.924
30	37.79	1.443	.00749	.1042	7.67	2.021	.952
48*	36.68	2.553	.01317	.1820	7.42	2.089	.985
31	Second Throat--		------	------	7.42	2.089	.985
32	35.43	3.917	.02016	.280	7.78	1.992	.939
33	34.52	4.827	.02472	.343	8.30	1.867	.879
34	33.44	5.907	.02513	.349	8.70	1.782	.840
35	30.97	8.377	.04289	.597	9.82	1.578	.743
36	28.45	10.897	.05580	.776	11.34	1.367	.644
37	26.66	12.687	.06496	.903	12.52	1.146	.540
38	26.12	13.187	.06752	.939	13.74	.985	.464
39	25.37	13.977	.07157	.994	22.56	.787	.371
40	25.28	14.067	.07203	1.000	28.18	.550	.259
41	25.40	13.947	.07141	.992	28.18	.550	.259
42	25.53	13.817	.07075	.983	28.18	.550	.259

Second Throat Area = 7.30 Square Inches

Before Second Throat, P_o = 95.89 psia; Reference = 39.253

After Second Throat, P_o = 95.89 psia; Reference = 39.347

*Pressure Taps on Centerbody

Part 5. CENTERBODY ADVANCED 0.1 INCH FROM

DESIGN OPERATING POSITION

TEST SECTION EMPTY

Station	Average Reading	Static Pressure in.hg.abs.	$\frac{P}{\bar{P}_o}$	$\frac{P}{\bar{P}_e}$	Area	$\frac{\bar{A}_1}{A}$	$\frac{A_o}{A}$
21	38.85	.407	.002095	.0294	16.34	.949	.438
22	38.85	.407	.002095	.0294	16.69	.929	.429
23	38.82	.437	.00225	.0315	16.93	.915	.423
24	38.85	.407	.002095	.0294	16.62	.933	.432
44 *	38.38	.877	.00451	.0631	16.38	.946	.438
25	38.85	.407	.002095	.0294	15.88	.976	.452
45 *	38.40	.857	.00441	.0617	14.30	1.084	.502
26	38.85	.407	.002095	.0294	14.22	1.090	.504
27	38.30	.957	.00493	.0692	11.97	1.295	.598
46 *	38.48	.777	.00400	.0560	10.85	1.429	.661
28	37.98	1.277	.00658	.0920	10.72	1.446	.668
29	36.77	2.487	.01280	.1793	8.25	1.879	.868
47 *	37.10	2.157	.01110	.1540	7.87	1.970	.912
48 *	36.68	2.577	.01326	.1870	7.32	2.117	.977
30	36.77	2.487	.01280	.1793	7.32	2.117	.977
31	Second Throat--		------	-----	7.17	2.162	1.000
32	36.57	2.687	.01383	.1938	7.69	2.016	.932
33	35.85	3.407	.01753	.245	8.22	1.886	.872
34	34.72	4.537	.02335	.328	8.72	1.778	.822
35	31.52	7.737	.03982	.558	9.76	1.588	.734
36	29.00	10.257	.05280	.740	11.32	1.369	.633
37	26.92	12.377	.06371	.892	13.29	1.166	.539
38	26.51	12.747	.06561	.919	15.51	1.000	.462
39	25.49	13.767	.07086	.992	23.0	.674	.312
40	25.38	13.877	.07143	1.000	28.18	.550	.254
41	25.50	13.757	.07081	.992	28.18	.550	.254
42	25.58	13.677	.07040	.986	28.18	.550	.254

Second Throat Area = 7.17 Square Inches

Reference = 39.257

P_o = 95.390 psia

*Pressure Taps on Centerbody.

Part 6. CENTERBODY ADVANCED 4.88 INCHES AHEAD OF DESIGN OPERATING POSITION

TEST SECTION EMPTY

Station	Average Reading	Static Pressure in.hg.abs.	$\frac{P}{P_o}$	$\frac{P}{P_e}$	Area	$\frac{A_1}{A}$	$\frac{A_2}{A}$
21	38.82	.431	.00216	.0210	16.40	.954	.313
22	38.82	.431	.00216	.0210	16.11	.945	.310
44*	38.18	1.071	.00537	.0520	15.82	.980	.322
23	38.80	.451	.00226	.0220	14.72	1.053	.346
45*	38.35	.901	.00452	.0390	13.71	1.131	.372
24	38.80	.451	.00226	.0220	12.75	1.216	.399
46*	38.40	.951	.00477	.0464	10.25	1.512	.497
25	37.78	1.471	.00738	.0718	10.08	1.538	.505
47*	36.55	2.701	.01355	.1318	7.30	2.123	.697
26	37.35	1.901	.00953	.0927	6.80	2.279	.748
48*	36.23	3.021	.01515	.1464	6.72	2.307	.759
27	36.60	2.651	.01330	.1293	6.12	2.533	.832
28	35.48	3.771	.01891	.1840	5.86	2.645	.869
29	35.33	3.921	.01967	.1912	5.34	2.903	.953
30	35.20	4.051	.02032	.1977	5.15	3.001	.985
31	Second Throat----		------	-----	5.09	3.045	1.000
32	28.83	10.401	.05216	.507	5.56	2.788	.915
33	25.27	13.961	.07002	.681	6.42	2.414	.793
34	22.40	16.731	.08391	.816	7.36	2.106	.692
35	19.90	19.331	.09695	.943	9.31	1.645	.541
36	19.48	19.751	.09906	.963	11.35	1.366	.448
37	18.71	20.521	.10292	1.000	19.18	.808	.265
38	18.63	20.401	.10232	.994	26.45	.586	.192
39	18.82	20.411	.10237	.994	28.18	.550	.181
40	18.78	20.451	.10257	.995	28.18	.550	.181
41	18.76	20.471	.10267	.996	28.18	.550	.181
42	18.76	20.471	.10267	.996	28.18	.550	.181

Second Throat Area = 5.09 Square Inches

Before Second Throat, Reference = 39.251; P_o = 97.90 psia

After Second Throat, Reference = 39.231; P_o = 97.90 psia

*Indicates Pressure Taps on Centerbody.

Part 7. DIFFUSER RETRACTED 5.97 INCHES FROM DESIGN OPERATING POSITION

Flat Plate Installed in Test Section

Station	Distance From Nozzle Throat - In.	Reading	Static Pressure in.Hg.abs.	$\frac{P}{P_o}$
1	2.86	35.50	3.374	.0171
2	3.86	36.78	2.094	.0106
3	4.88	37.33	1.544	.00783
4	5.87	37.76	1.114	.00565
5	6.86	37.81	1.064	.00539
6	7.86	37.97	.904	.00458
7	8.85	38.11	.764	.00387
8	9.87	38.21	..664	.00337
9	10.86	38.30	.574	.00291
10	11.86	38.33	.544	.00276
11	12.88	38.37	.504	.00256
12	13.87	38.39	.484	.00245
13	14.88	38.42	.454	.00230
14	15.88	38.42	.454	.00230
43*	19.00	38.42	.454	.00230
15	19.43	38.50	.374	.00190
44*	20.00	38.23	.644	.00326
16	20.57	38.45	.424	.00215
45*	21.50	38.45	.424	.00215
17	21.74	38.42	.454	.00230
18	22.84	38.37	.504	.00256
46*	23.00	38.45	.424	.00215
19	24.03	38.22	.654	.00331
47*	24.50	38.41	.464	.00235
20	25.17	37.68	1.194	.00606
48*	26.00	38.21	.664	.00337
21	29.62	37.10	1.774	.00900
22	32.62	36.61	2.264	.01148
23	35.62	36.02	2.854	.01447
24	37.62	35.27	3.604	.01776
25	39.62	34.70	4.174	.0021
26	41.62	33.05	4.824	.0245
27	43.52	33.25	5.674	.0288
28	44.42	32.90	5.974	.0303
29	45.99	32.37	6.504	.0330
30	46.46	32.14	6.734	.0372
31	46.62	32.19	6.684	.0339
32	47.62	32.03	6.844	.0347
33	48.62	31.93	6.944	.0352
34	49.62	31.78	7.094	.0359

*Pressure Taps on Flat Plate

Part 7 continued

Station	Distance From Nozzle Throat - In.	Reading	Static Pressure in.hg.abs.	$\frac{P}{P_o}$
35	51.62	31.81	7.064	.0358
36	53.62	31.92	6.9[illegible]4	.0352
37	55.62	31.68	7.1[illegible]4	.0365
38	57.62	31.49	7.3[illegible]4	.0374
39	60.62	31.39	7.484	.0379
40	63.62	31.38	7.494	.0380
41	68.62	31.03	7.844	.0397
42	72.62	31.02	7.854	.0398

Second Throat Area = 13.00 Square Inches

Reference = 38.874; P_o = 98.6 psia

Part 8. END PRESSURES FOR VARIOUS RUNNING TIMES

Running Time Seconds	P_e in. hg. abs.	P_o psia	$\frac{P_e}{P_o}$	Source
0	1	95.8	.0050	Initial Conditions
38	10.1	94.4	.0525	Part 2 Station 41
46	12.8	96.9	.0520	Recorded After Shut Down
46	13.9	95.7	.0711	Part 1 Station 40
50	13.4	96.9	.0679	Recorded After Shut Down
50	13.8	96.4	.0703	Recorded After Shut Down
52	12.4	90.4	.0674	Recorded After Shut Down
52	13.4	96.4	.0683	Recorded After Shut Down
84	20.47	97.9	.1027	Part 6 Station 42
87	20.8	97.4	.1038	Recorded After Shut Down.

Part 9. GENERAL PERFORMANCE DATA FOR VARIOUS CENTERBODY LOCATIONS

Centerbody Location[1]	Max. Area Ratio, A_1/A_9	Running Time Seconds	Pressure Ratio, P_o/P_e (from Fig. 9)	Pressure Ratio Req'd to operate P_e/P_o	Remarks
-2.00	1.72	32	.046	21.6	Tunnel Empty
-1.00	1.92	40	.055	18.1	Tunnel Empty
0.00	2.14	46	.062	16.1	Tunnel Empty
+0.40	2.18	50	.067	15.0	Tunnel Empty
+0.50	2.19	52	.069	14.5	Tunnel Empty
+0.60	2.20	52	.069	14.5	Tunnel Empty
+0.64	2.21	50	.067	15.0	Tunnel Empty
+1.50	2.33	56	.073	13.7	Tunnel Empty
+2.50	2.50	68	.086	11.6	Tunnel Empty
+4.00	2.82	75	.093	10.8	Tunnel Empty
+4.88	3.03	84	.102	9.8	Tunnel Empty
+4.88	3.03	87	.104	9.6	Tunnel Empty
0.00	2.13	35	.049	25.6	Survey Rake Installed
0.00	2.13	22	.033	30.3	0.095" Dia. Tube 2 1/2 inch penetration
0.70	2.22	30	.043	23.3	0.095" Dia. Tube 1 3/4 inch penetration
4.88	3.03	60	.078	13.0	0.095" Dia. Tube 1 inch penetration

P_o = 95.8 psia; T_o = 60°F

Initial Vacuum Tank Pressure = 1 inch of mercury

[1](inches ahead or designed operating position)

TABLE IV LOCATION OF STATIC PRESSURE TAPS

1. TAPS ON SHELL

Station Number	Distance From Lip of Diffuser Inches	Distance From Nozzle Throat Inches	Inside Diameter of Shell Inches
21	3.00	29.62	4.561
22	6.00	32.62	4.610
23	9.00	35.62	4.659
24	11.00	37.62	4.691
25	13.00	39.62	4.721
26	15.00	41.62	4.757
27	16.90	43.52	4.787
28	17.80	44.42	4.801
29	19.37	45.99	4.827
30	19.84	46.46	4.835
31	20.00	46.62	4.838
32	21.00	47.62	4.956
33	22.00	48.62	5.073
34	23.00	49.62	5.191
35	25.00	51.62	5.426
36	27.00	53.62	5.662
37	29.00	55.62	5.897
38	31.00	57.62	6.132
39	34.00	60.62	6.250
40.	37.00	63.62	6.250
41	42.00	68.62	6.250
42	46.00	72.62	6.250

2. TAPS ON CENTERBODY

Number	Distance From Base of Cone (Measured Along Surface) Inches	Diameter of Centerbody Inches
44	8.10	1.091
45	5.08	2.090
46	1.22	3.363
47	0.352	3.649
48	0.029	3.774

FIG. 1 PHOTOGRAPH OF DIFFUSER ASSEMBLY

The Centerbody is Installed in Starting Position, And The Outer Shell is Suspended Below.

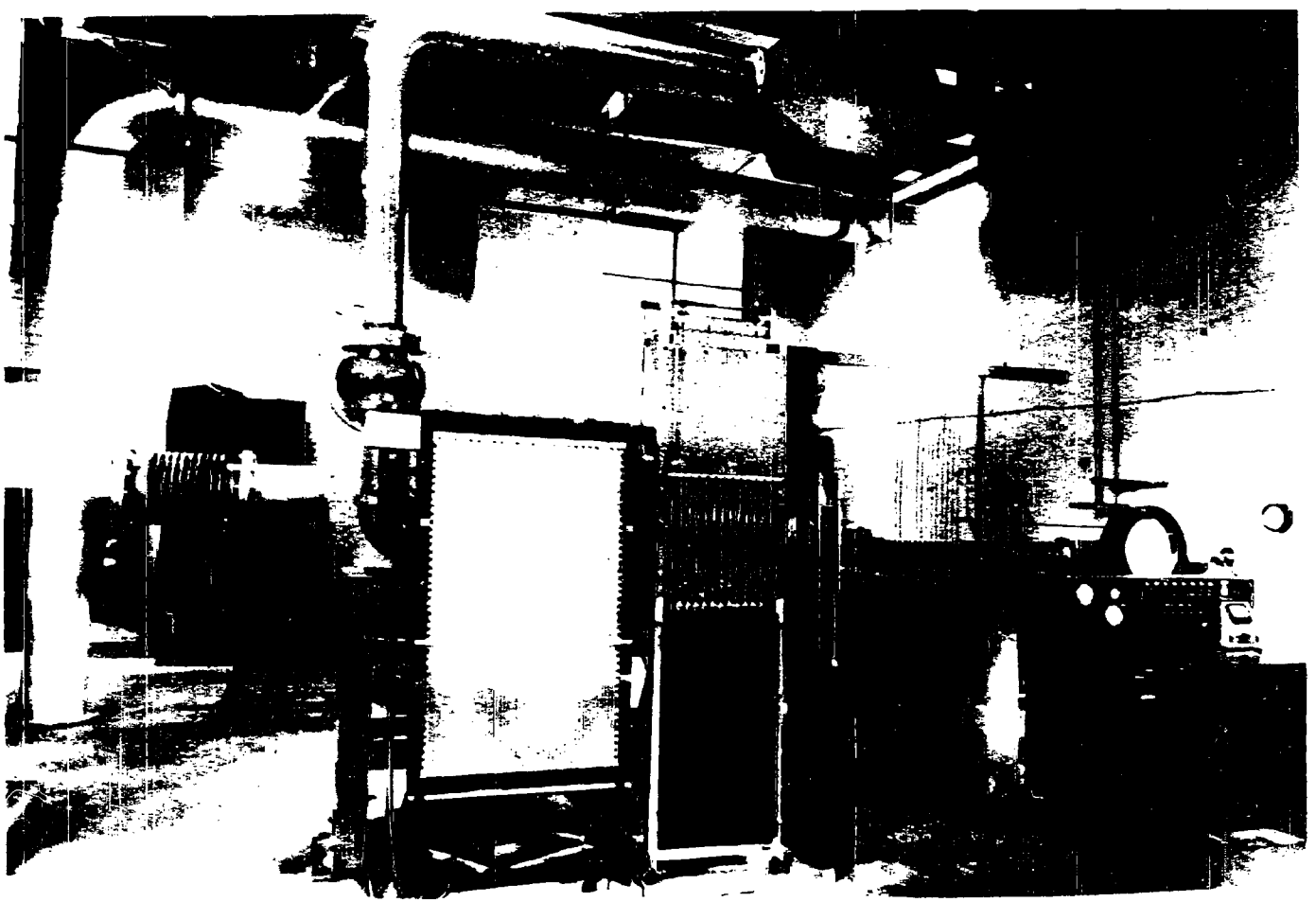

PHOTOGRAPH OF TUNNEL WORKING SECTION AND INSTRUMENTS

At The Extreme Right Are The Control Rope And Pressure Gauge
Just To The Left Of Centre Is The Early Type Manometer Board

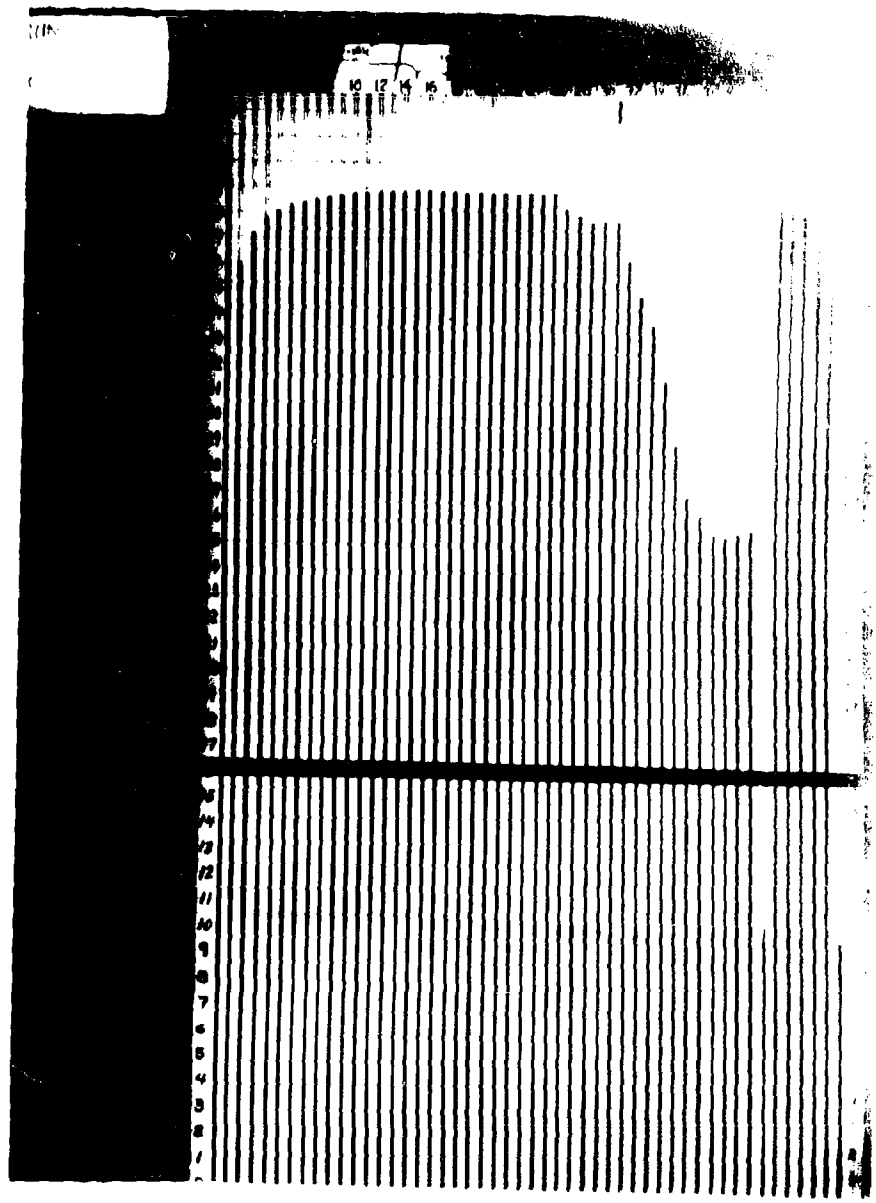

FIG. 3 TYPICAL PHOTOGRAPH OF MANOMETER BOARD

Centerbody In Design Operating Position Tube Numbers Correspond To Stations (Fig. 20 & 21) Tubes 43 And B (At The Extreme Right) Are Atmosphere Pressure Tube R (At The Extreme Left) Is The Reference Vacuum

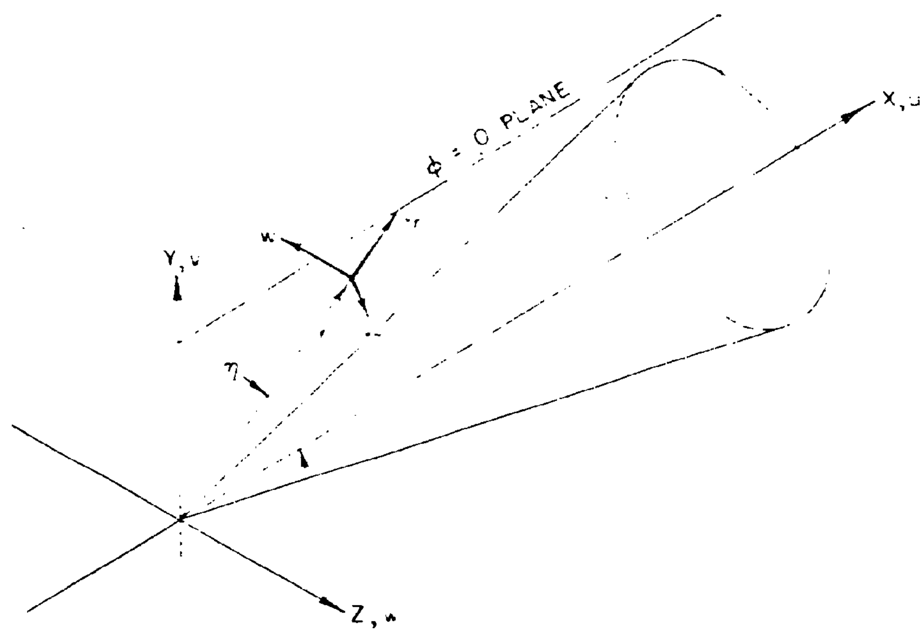

FIG 4 – COORDINATE SYSTEMS

ORL – UT
DWG AA 1627
JBK – CLW
1 – 25 – 56

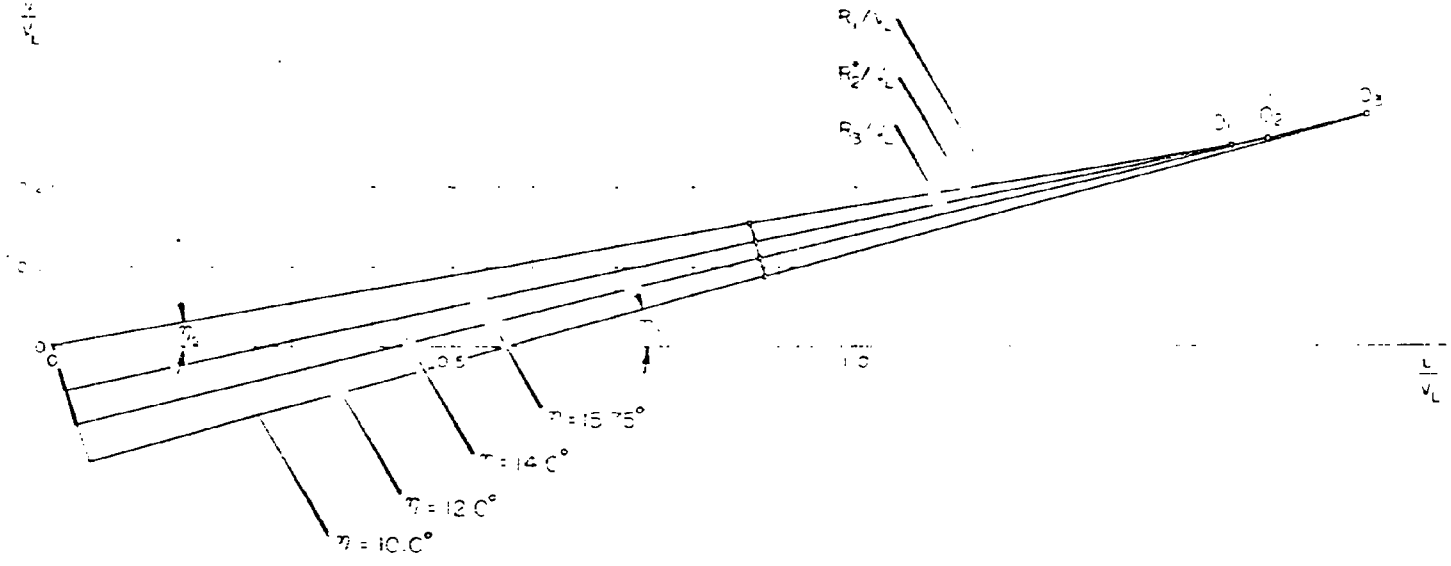

FIG. 5 – HODOGRAPH OF FLOW IN CONICAL REGION

ORNL – UT
DWG AA 1628
JBK – CLW
1 – 25 – 56

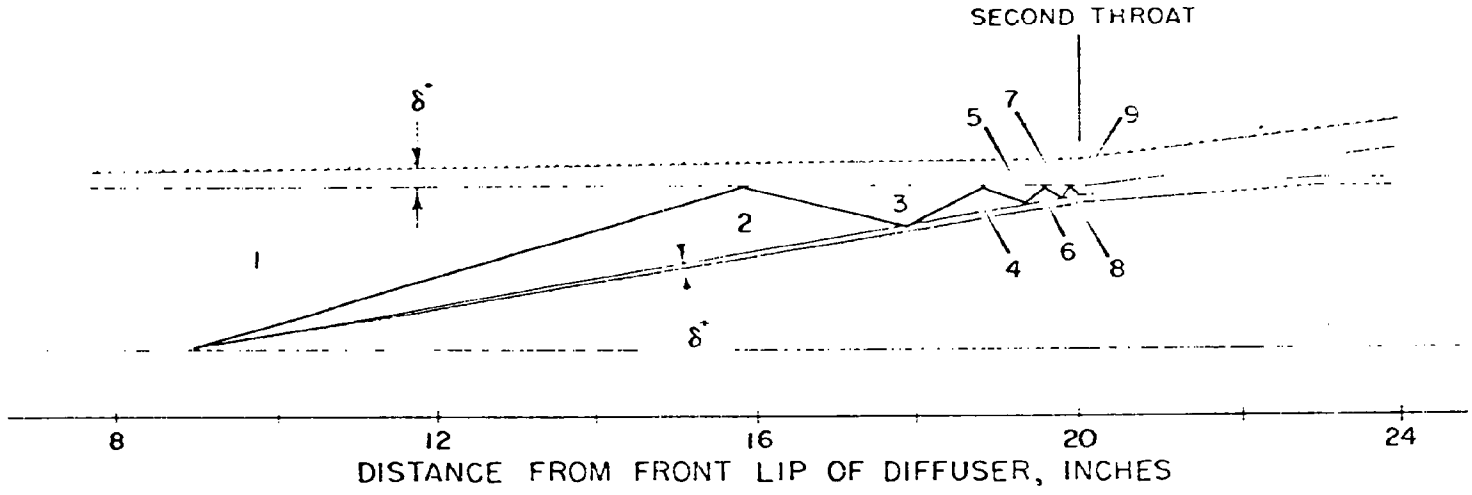

FIG. 6 – HALF SCALE SECTION OF DIFFUSER SHOWING THEORETICAL SHOCK PATTERN.

CENTERBODY IN DESIGN OPERATING POSITION. $M_1 = 4.89$.

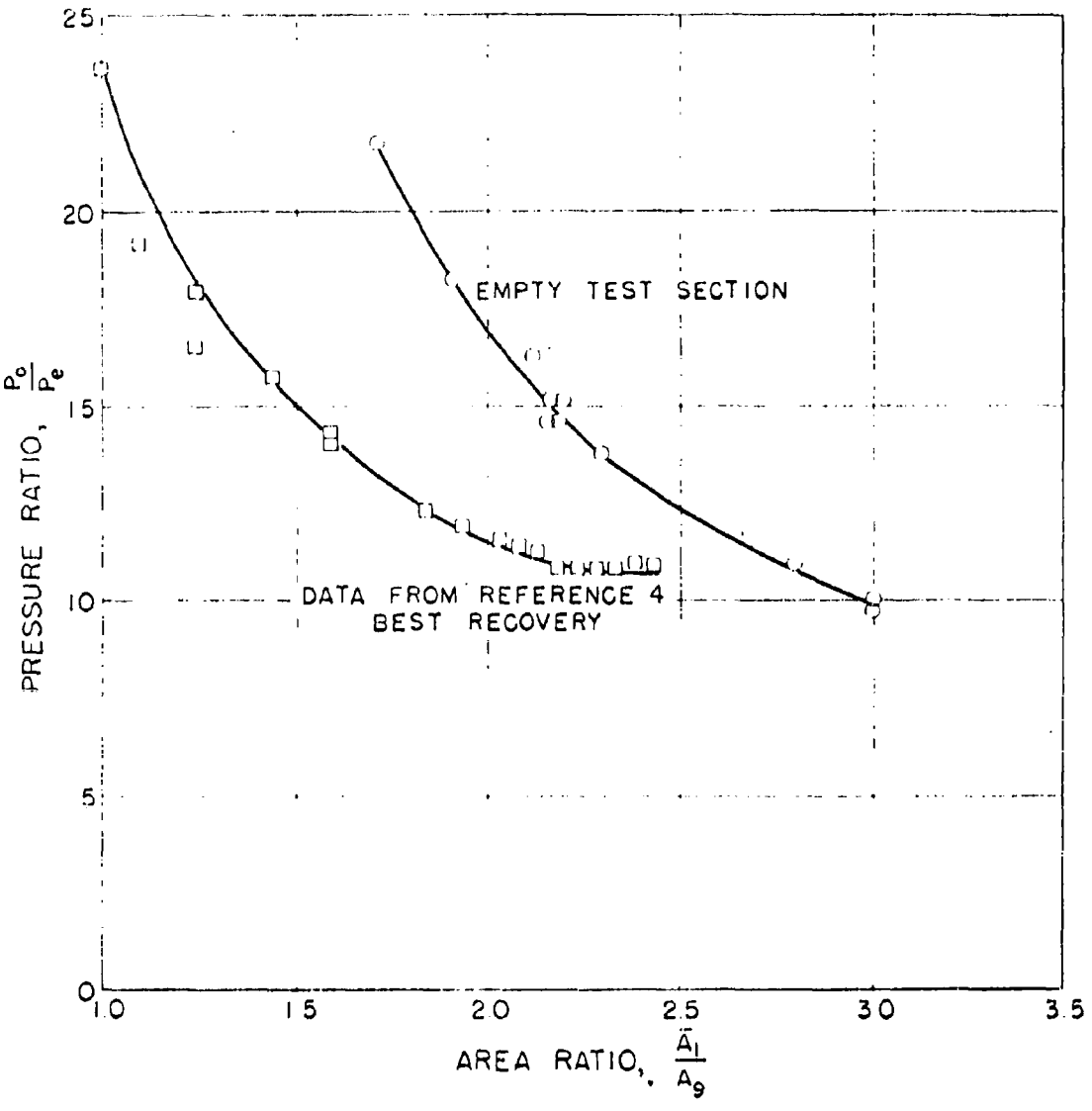

FIG. 7 – EFFECT OF SECOND THROAT AREA RATIO ON PRESSURE RATIO REQUIRED TO OPERATE

UHL – UT
DWG AA 1630
JBK – CLW
1 – 24 – 56

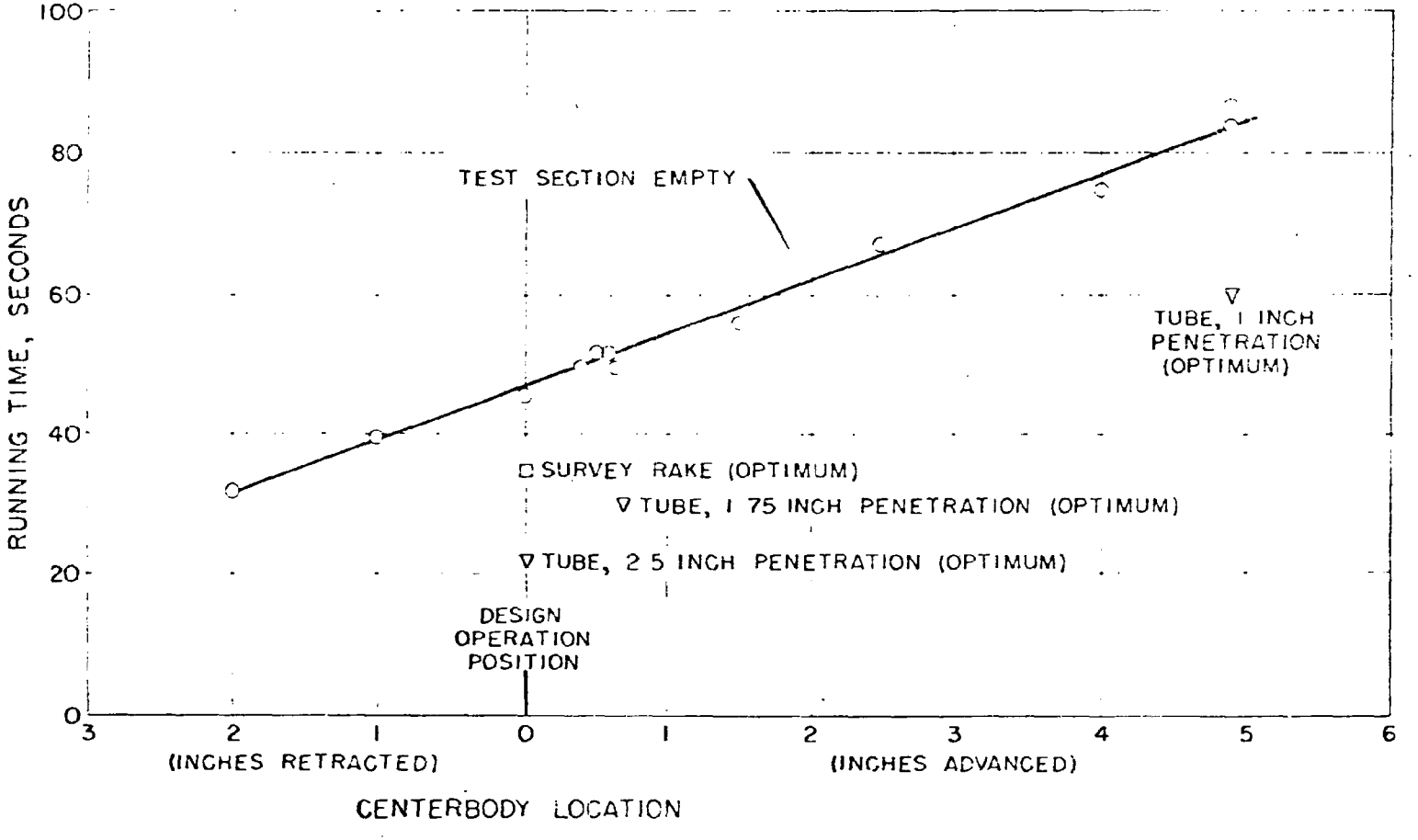

FIG. 8 – EFFECT OF CENTERBODY LOCATION ON RUNNING TIME

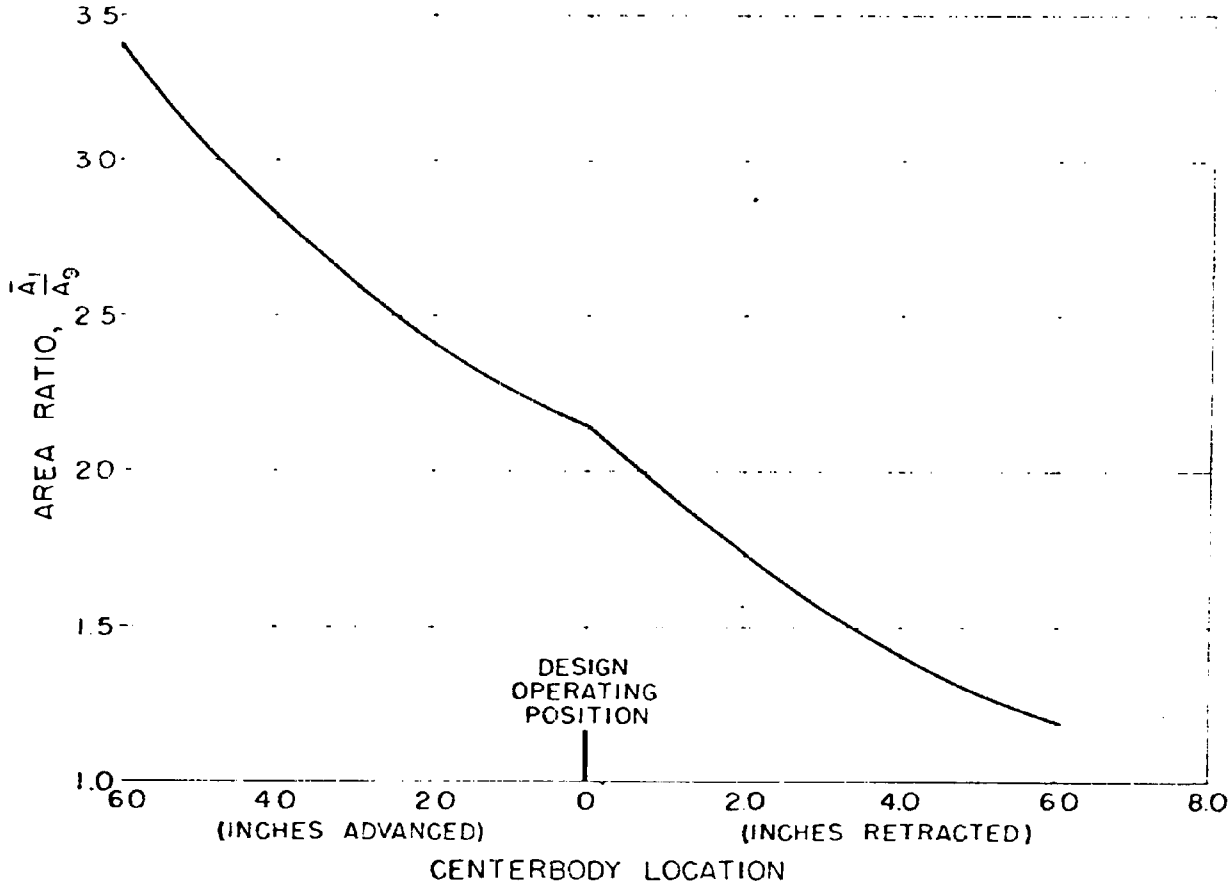

FIG. 9 – AREA RATIO VS. CENTERBODY LOCATION

DRL – UT
DWG AA 1632
JBK – CLW
1-24-56

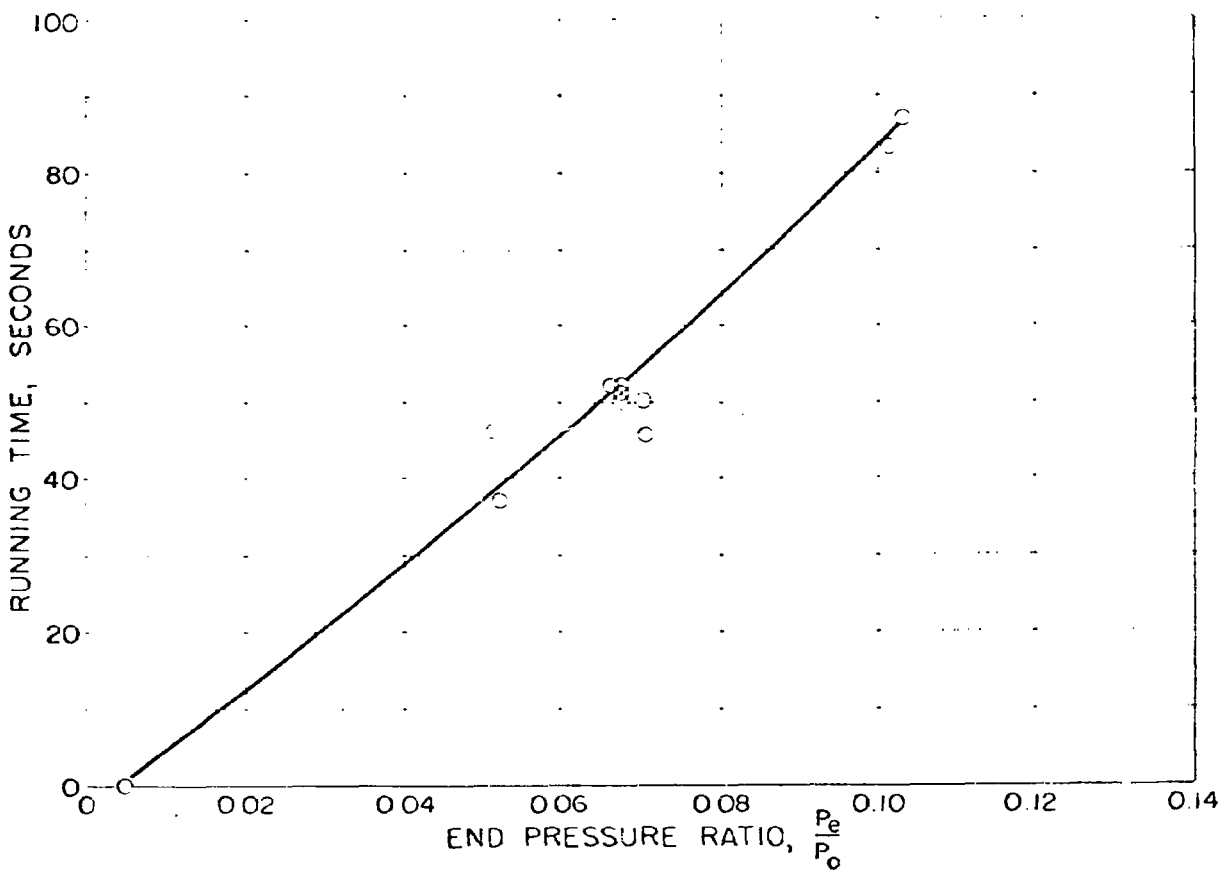

FIG. 10—EFFECT OF RUNNING TIME ON END PRESSURE RATIO. INITIAL CONDITIONS: P_e = 1 INCH HG, P_o = 95.8 PSIA.

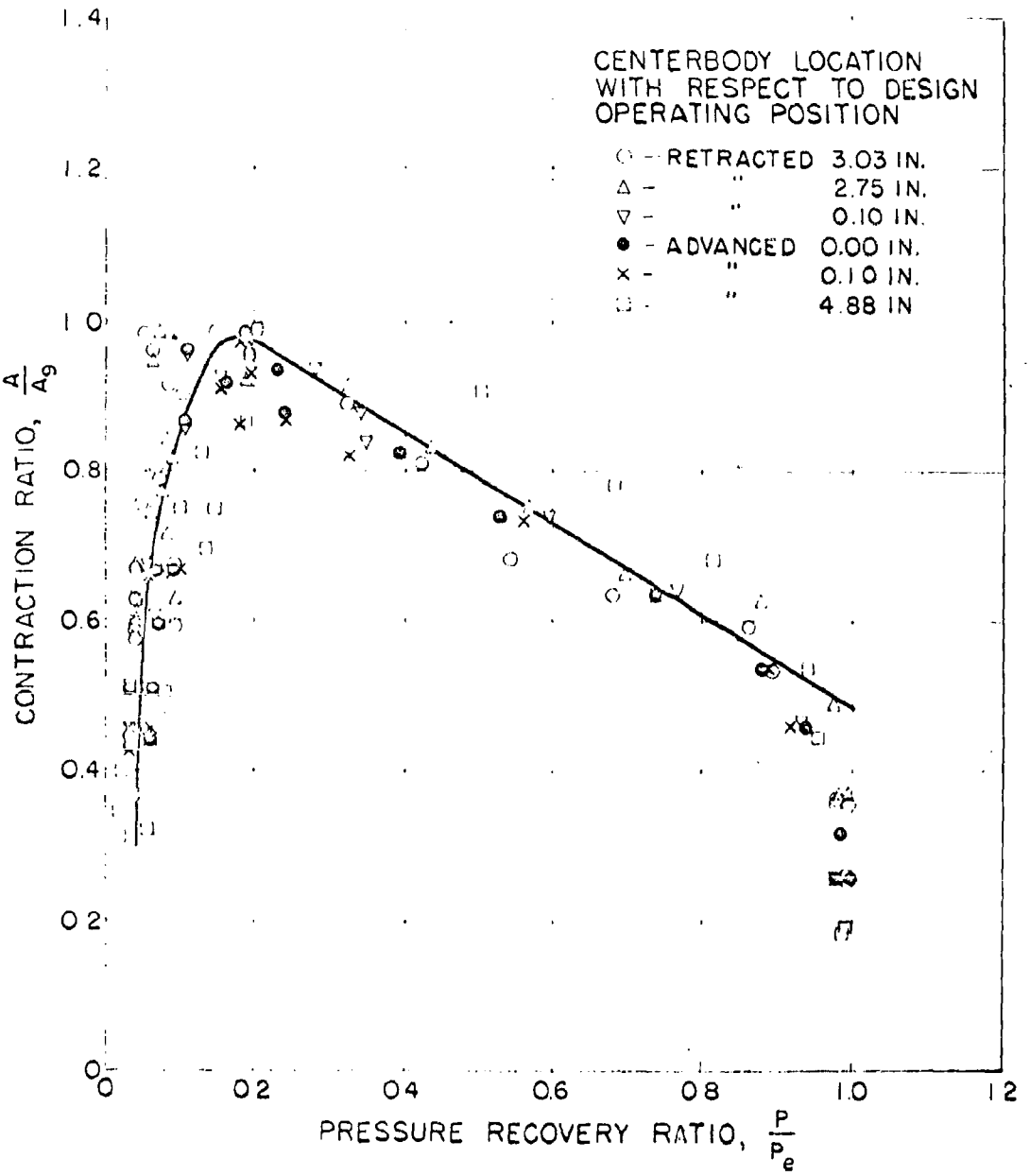

FIG. 11 – PRESSURE RECOVERY RATIO VS. CONTRACTION RATIO

DRL – UT
DWG AA 1634
JBK – CLW
2 – 6 – 56

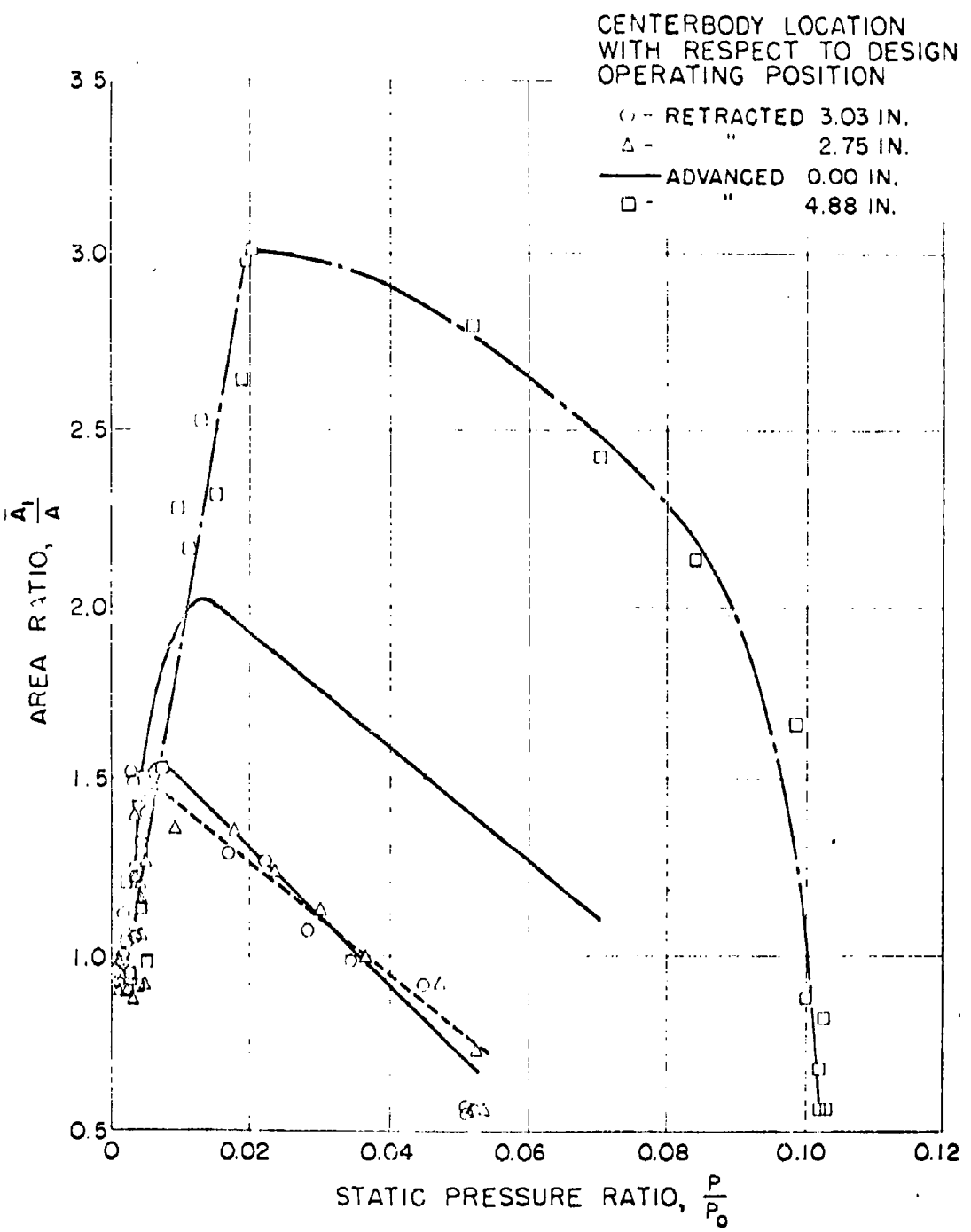

FIG. 12 - PRESSURE RATIO VS. AREA RATIO
TEST SECTION EMPTY

DRL - UT
DWG AA 1635
JBK - CLW
2 - 6 - 56

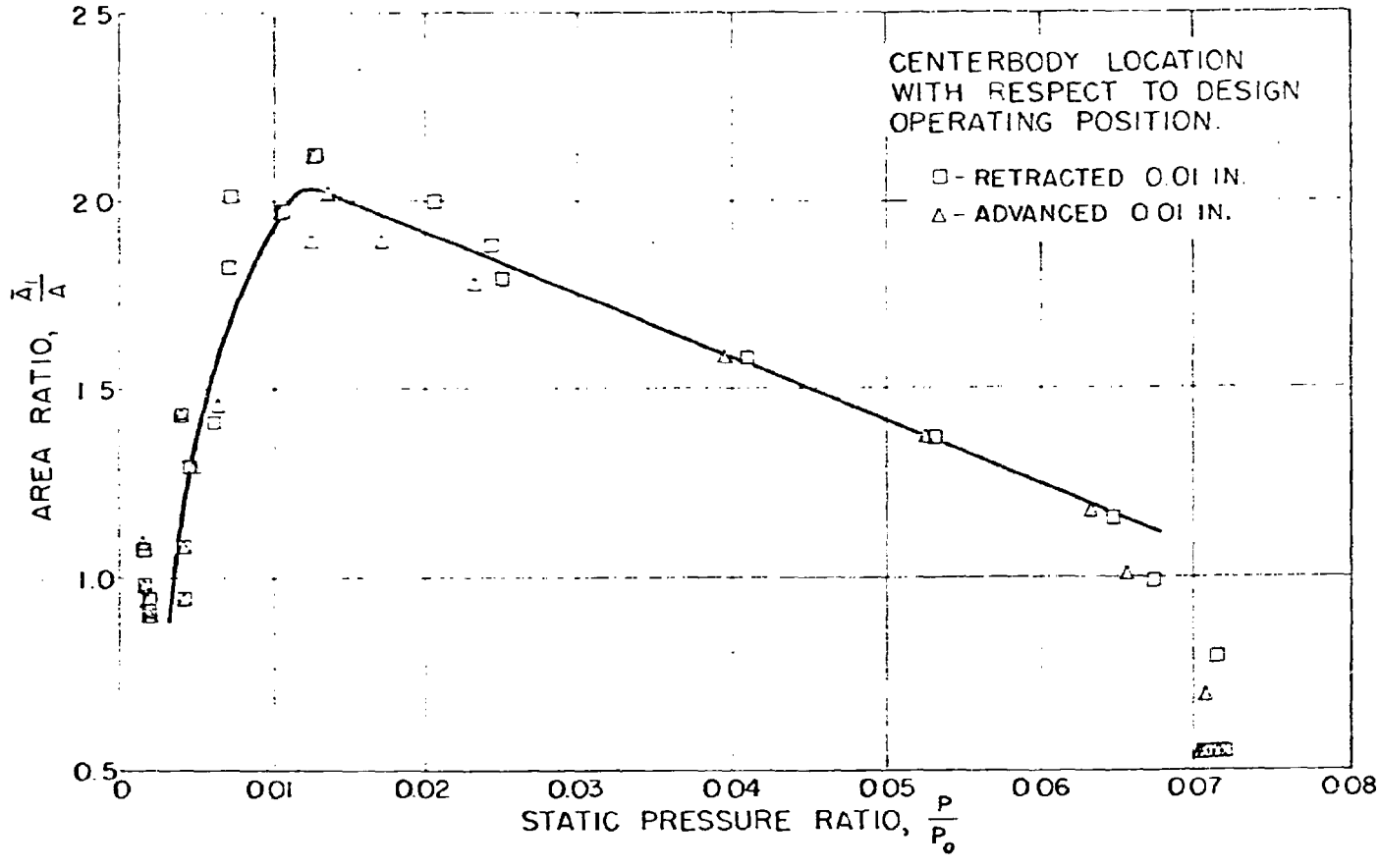

FIG. 13 - PRESSURE RATIO VS. AREA RATIO
TEST SECTION EMPTY

ORNL - LT
DWG AA 1636
JBK - CLW
1 - 25 - 56

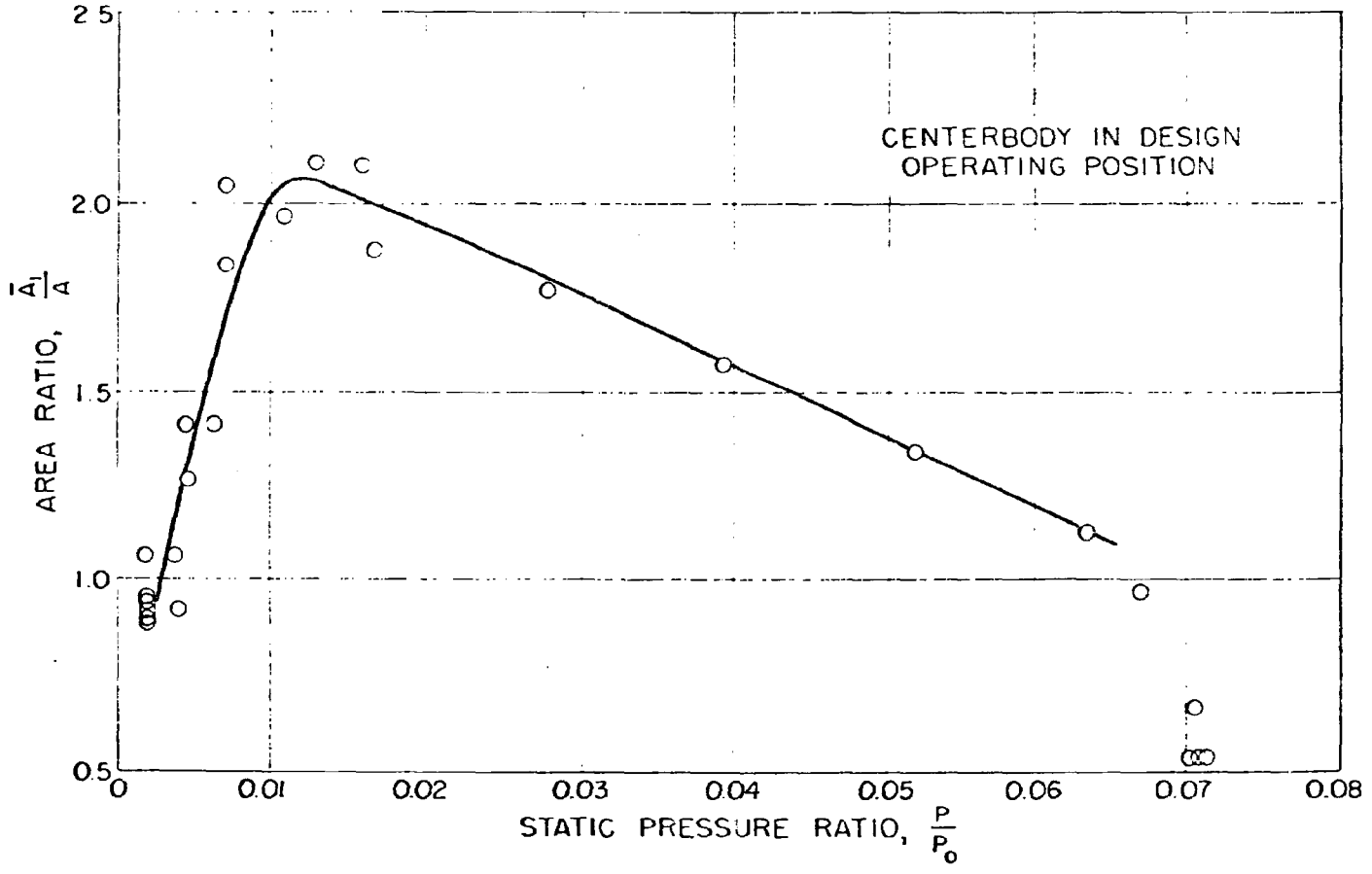

DRL - UT
DWG AA 1637
JBK - CLW
1 - 24 - 56

FIG. 14 - PRESSURE RATIO VS. AREA RATIO
TEST SECTION EMPTY

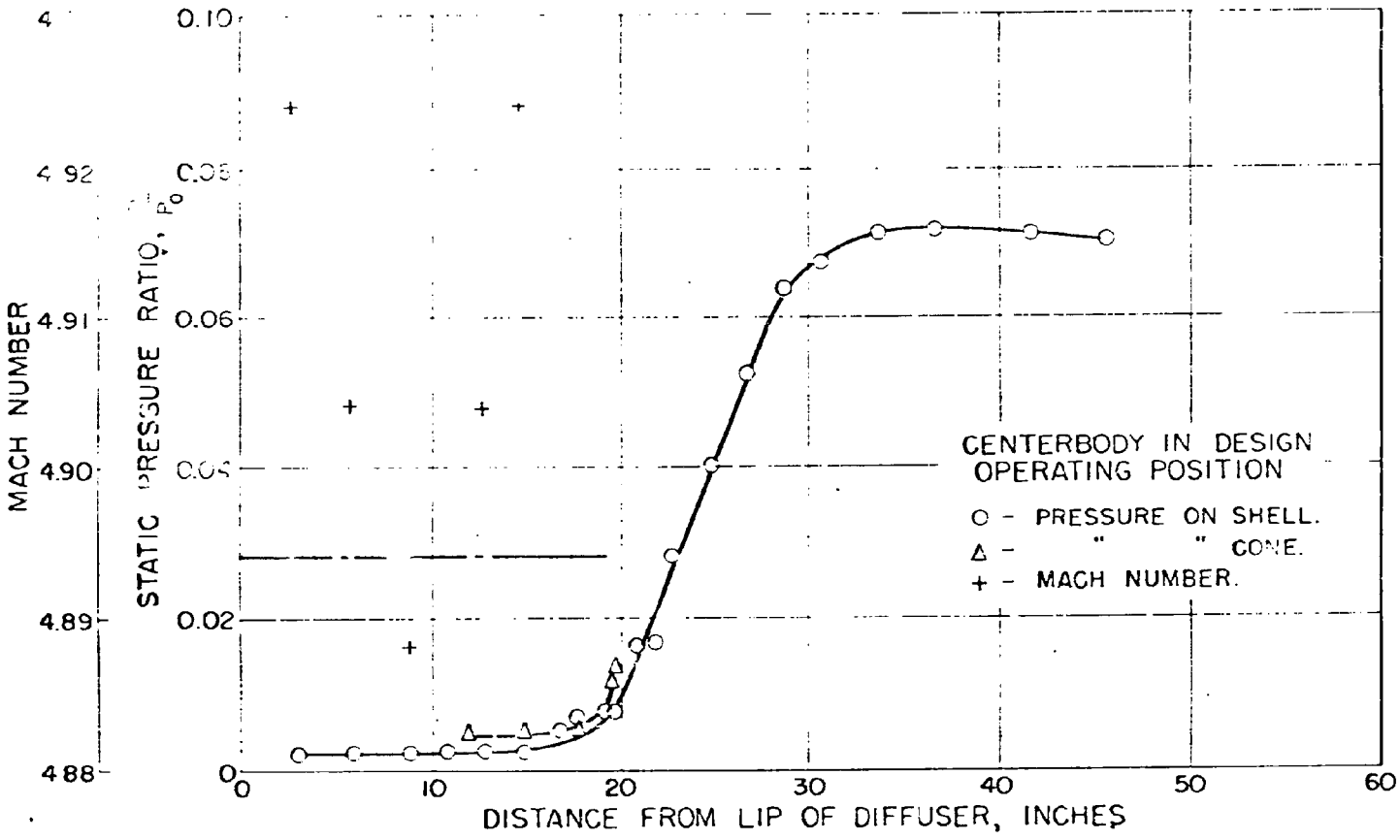

FIG. 15 - PRESSURE RATIO AND MACH NUMBER ALONG LENGTH OF DIFFUSER

ORNL - UT
DWG AA 1638
JBK - C.W.
1-24-56

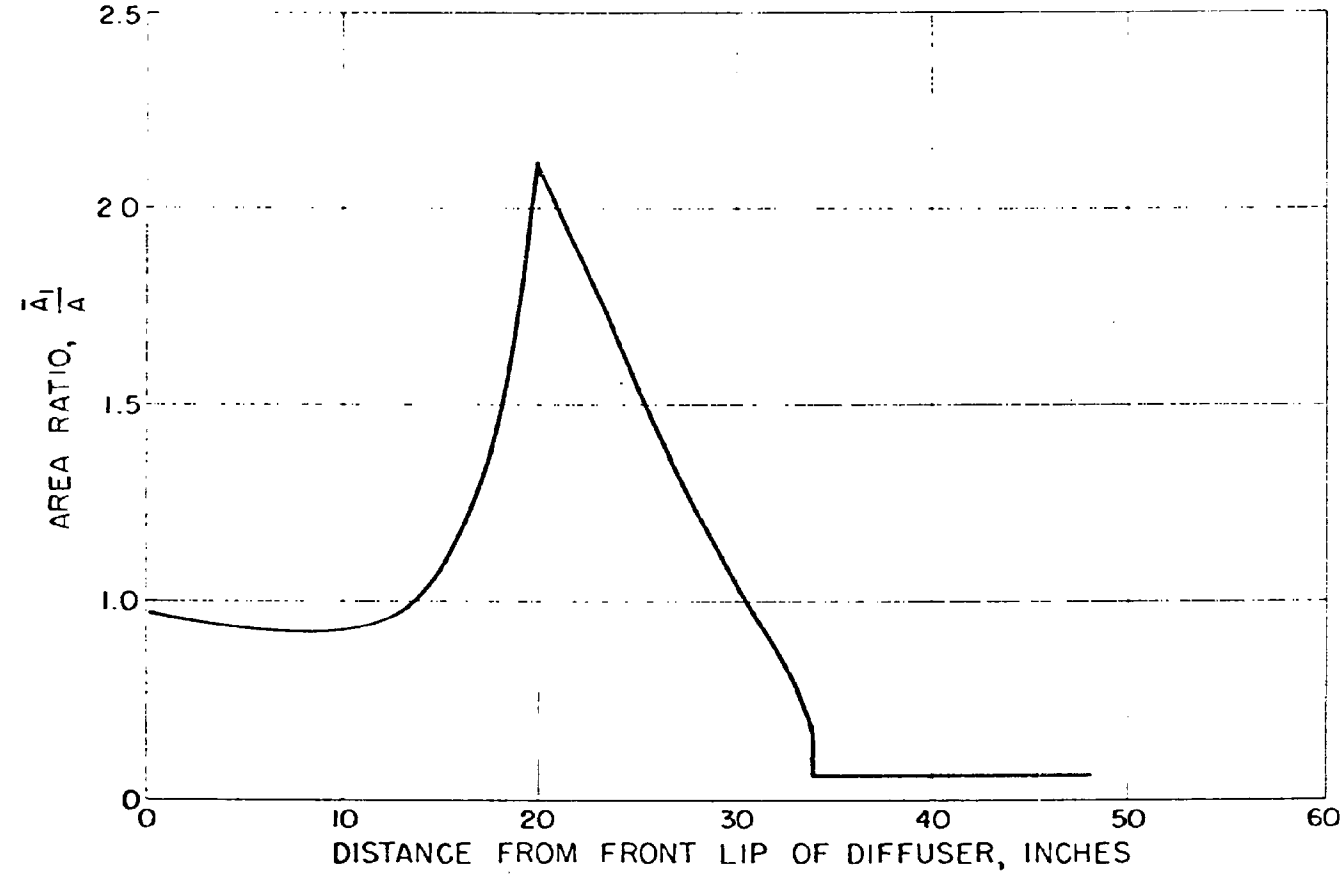

FIG. 16 - AREA RATIO ALONG DIFFUSER.
CENTERBODY IN DESIGN OPERATING POSITION.

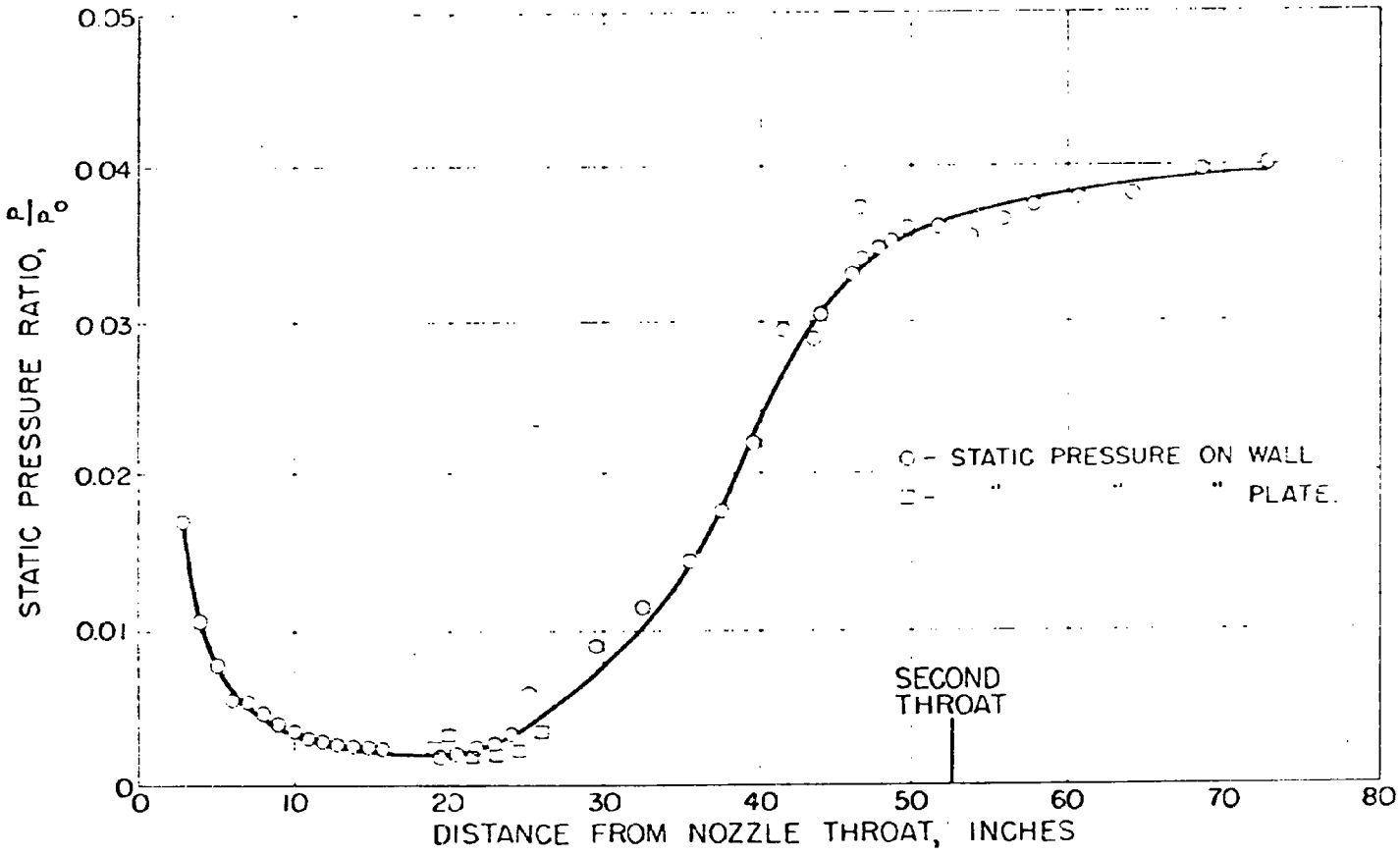

FIG. 17 – PRESSURE RATIO ALONG LENGTH OF WORKING SECTION.
FLAT PLATE IN TEST SECTION.

DHL – UT
DWG AA 1640
JBK – CLW
1 – 23 – 56

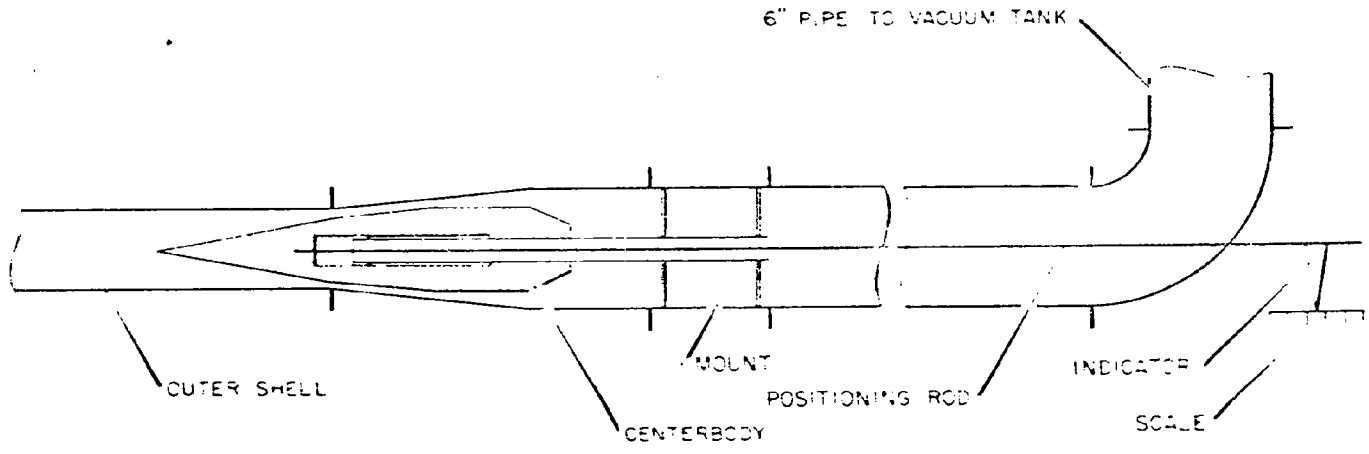

APPROXIMATELY $\frac{1}{10}$ TH SCALE

FIG. 18 – DIAGRAM OF DIFFUSER ASSEMBLY AND POSITIONING MECHANISM

ORNL - UT
DWG. A-1641
JBK - CLW
1 - 23 - 56

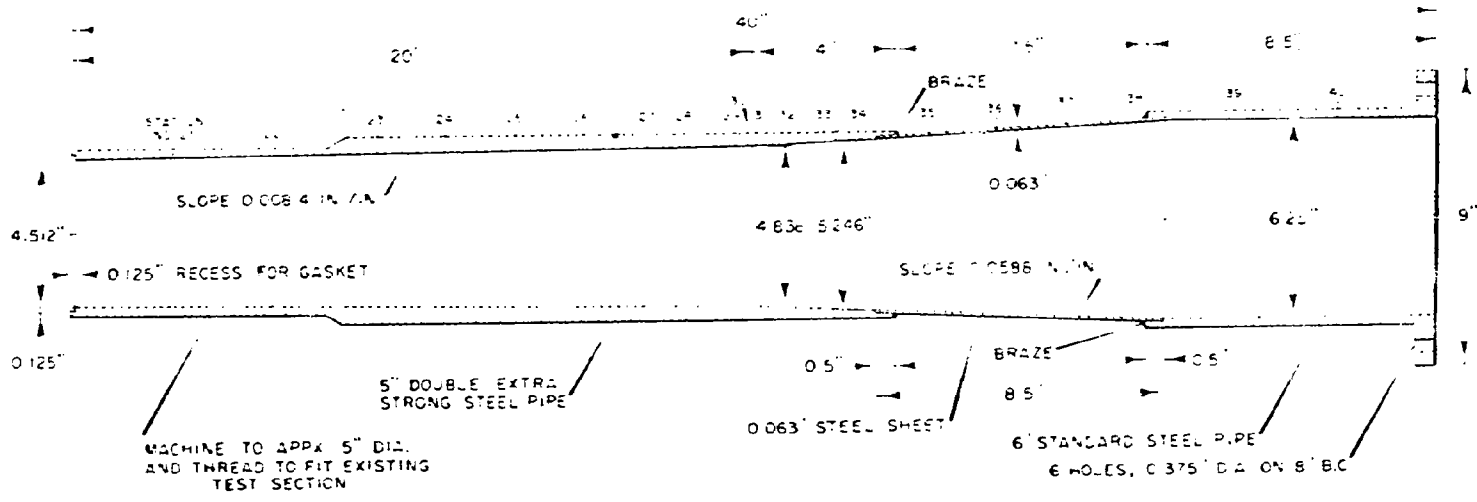

FIG. 19 – DETAIL DRAWING OF OUTER SHELL
FIFTH SCALE – LONGITUDINAL SECTION

CH. - CUT
DWG. AD. 1642
JHK - CLW
1 - 20 - 56

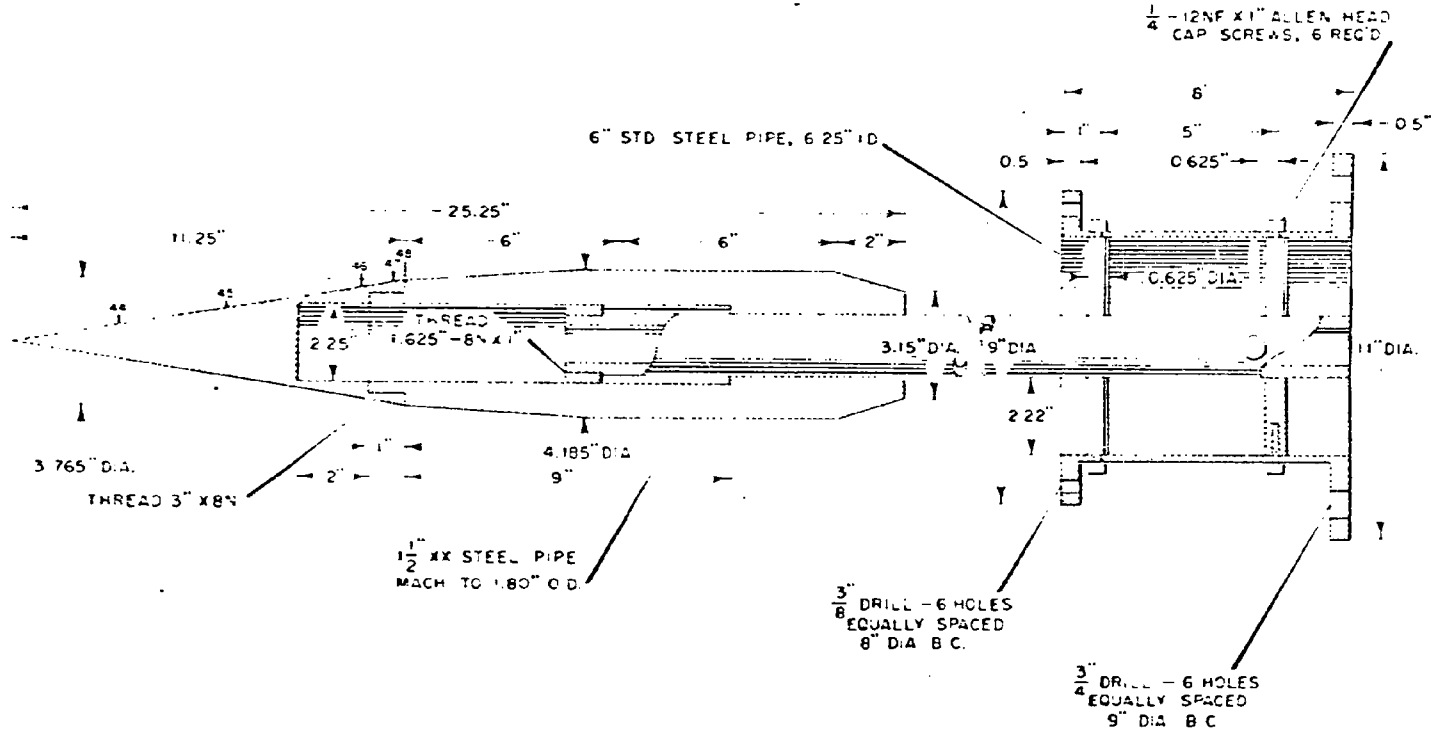

FIG. 20 – DETAIL DRAWING OF CENTERBODY
FIFTH SCALE – LONGITUDINAL SECTION

ORL - UT
DWG AA 1643
18X - CLW